ABSTRACT

PADMANABHAN, AADITYAA. Fault Location on Distribution Feeders. (Under the direction of Dr. Mesut E. Baran.)

Over the past decade feeder monitoring projects have gained momentum within the electric utility industry as more and more utilities find their installation useful and the price of these units becomes cheaper. These monitoring units relay data back to the central control center through dedicated optic fiber links or wireless networks. As such meters are incorporated into the system; more real time data becomes available for controlling and monitoring the system. One such application is locating where faults occurred on the system using this data. The thesis presents a method that uses the current waveforms from a few locations on the feeder and processes them to find the exact location of a permanent fault on the distribution feeder once it occurs.

Fault Location on Distribution Feeders

by
Aadityaa Padmanabhan

A thesis submitted to the Graduate Faculty of
North Carolina State University
in partial fulfillment of the
requirements for the Degree of
Master of Science

Electrical Engineering

Raleigh, North Carolina

2012

APPROVED BY:

Dr. Subhashish Bhattacharya	Dr. Sdrjan Lukic

Dr. Mesut E. Baran
Chair of Advisory Committee

BIOGRAPHY

Aadityaa Padmanabhan was born in Mumbai, India on the 10th of August, 1988. He completed high school in Mumbai before moving to Chennai, India to pursue a Bachelors degree in Electrical and Electronics Engineering at Sri Sivasubramaniya Nadar College of Engineering (affiliated to Anna University, Chennai.) Up on graduation in 2010, he enrolled at North Carolina State University for his Masters degree in Electrical Engineering. Since then then he has been working under the guidance of Dr. Mesut E. Baran.

ACKNOWLEDGEMENTS

I wish to express my gratitude to the following people who have helped and guided me throughout my thesis, and stood by me throughout my course of study

To my advisor, Dr. Mesut Baran, for his continued guidance throughout the course of my graduate studies. My efforts would have been for naught were it not for his support and instruction.

To all my colleagues at the FREEDM Systems Center, who I became good friends with over the period of my stay with them.

To my fellow students at the University who made these two years fun and something I would never forget.

To my family back in India who have always guided and supported me in all my endeavours.

TABLE OF CONTENTS

LIST OF TABLES

LIST OF FIGURES

Chapter 1 Introduction

Over the past decade feeder monitoring projects have gained momentum within the electric utility industry as more and more utilities find their installation useful and the price of these units becomes cheaper. These monitoring units relay data back to the central control center through dedicated optic fiber links or wireless networks. As such meters are incorporated into the system; more real time data becomes available for controlling and monitoring the system. One such application is locating where faults occurred on the system using this data. The thesis presents a method that uses the current waveforms from a few locations on the feeder and processes them to find the exact location of a permanent fault on the distribution feeder once it occurs.

1.1 Background

Formerly, most fault location studies were performed primarily on the transmission networks as these are the systems that carry the bulk power and therefore any interruptions on these proved highly detrimental to the operation of the system. The fault location techniques devised for these systems are usually not directly applicable to the distribution system due to a variety of factors. At the transmission level many metering points are available and that make analyses on the transmission network comparatively easy. On the other hand, the distribution networks have very few measurements associated with them, if any. Therefore any form of analysis on these networks becomes difficult. Also, due to these differences analysis methods from the transmission side cannot be directly ported to the distribution networks.

1.2 Literature Review

Various fault location techniques currently in practice were reviewed. These range from simple techniques that use simple fundamental frequency current values and waveforms to those that

employ travelling waves and high frequency techniques to locate the fault.

Glenn C. Lampley et. al propose a method in [5] whereby short-circuit analysis is used to pre-calculate the fault currents at all the locations in the system and then these values are used to locate the fault based by comparing the observed fault current magnitude with the calculated values on the occurrence of the fault. The occurrence of a fault and its type is determined by checking the measured current with the threshold current for each of the three phases and the neutral. The steady state fault current is calculated from the measured substation waveform. Likely locations are ranked based on the closeness of their match with the value from the short circuit analysis.

M. M. Saha, D. Novosel and others outline the various fault location techniques that are primarily used on the distribution system [8]. One approach uses already available data from the existing distribution automation system to locate the fault. It bases its estimate on the measured fault current magnitude at say a microprocessor based relay and compares it to the calculated fault current magnitude at that point. Locations are estimated based on the matches between the observed and the measured fault current magnitudes. Algorithm of Saha et al. [6] uses the fundamental component of the currents and voltages measured before and during the fault. The pre-fault and fault loop impedances are calculated from these values. This data is then used to locate the fault.

The book Fault Location on Power Networks [7] by M. M. Saha et. al. presents the various fault location techniques available for power networks and how these can be applied to distribution networks. It explains phasor-based algorithms, one-end, two-end and multi-end impedance-based fault location algorithms and artificial intelligence based algorithms and how these are applied to the networks for the various faults that occur on the system. It further goes on to explain how these techniques may be applied to the distribution system with some

modifications.

The fault location technique by S. Das et. al [9] is one where faults are simulated at every bus on the distribution feeder circuit model. The fault current is then plotted against the distance to the fault. When a fault occurs, the fault current from the measurement device is extrapolated on the graph to obtain estimates as to the location of the fault. As the feeder circuit model is used, the actual system load and the non-uniform line impedances are taken into account while forming the short circuit current profile.

1.3 One-End Impedance-based Fault Location [7]

Consider figure 1.1. If a fault occurs at a distance from the point of measurement on a line, the distance can be calculated provided the voltage and the current at the time of the fault can be determined. This data is obtained by placing meters at the point of measurement (namely at the substation breaker). Neglecting the line charging currents,

$$Z_F = \frac{V_F}{I_F} = dZ_L + R_F \tag{1.1}$$

R_F is the fault resistance. Z_L is the impedance of the line per unit length. From the above equation, the distance to the fault can be estimated as

$$d = \frac{imag(Z_F)}{imag(Z_L)} \tag{1.2}$$

R_F is always a pure resistance and therefore this technique can be used to provide an accurate estimate of the distance to the fault.

This is the basic idea behind all impedance based fault location techniques.

This technique is usually best suited for radial networks and therefore works well with dis-

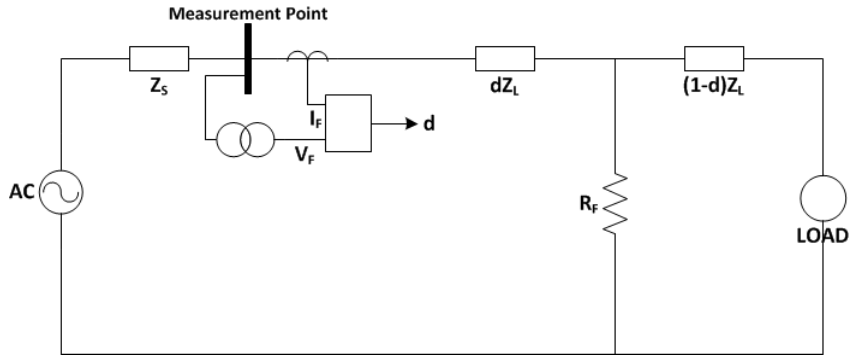

Figure 1.1: One End Impedance Based Fault Location

tribution networks that have just once source of power and the rest are all loads. Therefore there is only one source feeding the fault in the system.

This basic technique has the drawback that as different conductor types are included into the system the impedance becomes non-linear. Also, the taps on the distribution feeder add to the inaccuracy in estimation.

1.4 Artificial Intelligence based Fault Location

Artificial intelligence based methods can be broadly classified into three broad categories [7] expert system techniques, artificial neural networks and fuzzy-logic systems.

Expert system techniques consist of a set of knowledge rules based on a heuristic approach that are stored as If then statements. The inference engine uses these rules and the available data to draw out conclusions and come up with an estimate as to the location of the fault. These rules follow the basic thought process followed by a human being, in this case an operator at the control center.

The Figure 1.2 shows the block diagram for an Expert System. Almost all applications of the Expert Systems are off-line tasks such as fault diagnosis [1], classification of faults [4] and

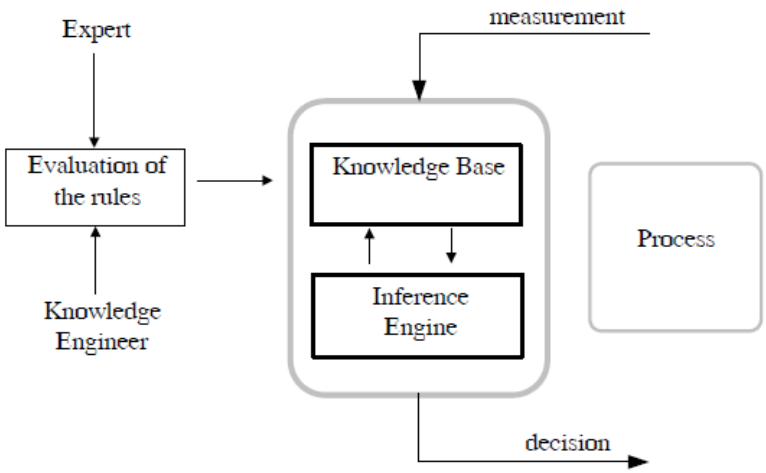

Figure 1.2: Simplified Block Diagram of an Expert System

faulted section identification [3].

Figure 1.3 shows the simplified block diagram for a fuzzy logic based system. The process in the case of fault location in the feeder on which the fault occurs. Fuzzy logic techniques make soft relationships between events and their corresponding causes/measurements. Unlike traditional mathematics where variables only take numerical values, fuzzy logic allows for linguistic definitions within the logic. These kinds of definitions let descriptions to be graded instead of being a true-false relationship. This allows a technique to come to conclusions based on ambiguous, incomplete, imprecise and vague data. The process of *fuzzyfication* allows for data and measurements to account for errors that might occur during communication and/or measurement. This *fuzzyfied* data is then used in a mathematical model to find the position of the fault. The fuzzy logic based system looks very similar to the expert system. However, compared to the expert system, the fuzzy logic system has a fewer number of rules.

Artificial neural networks do not rely on a set of rules unlike the expert system technique. ANNs are trained on data or actual cases. This training means that the program keeps learning as more cases are run through it. Therefore the program runs better with time.

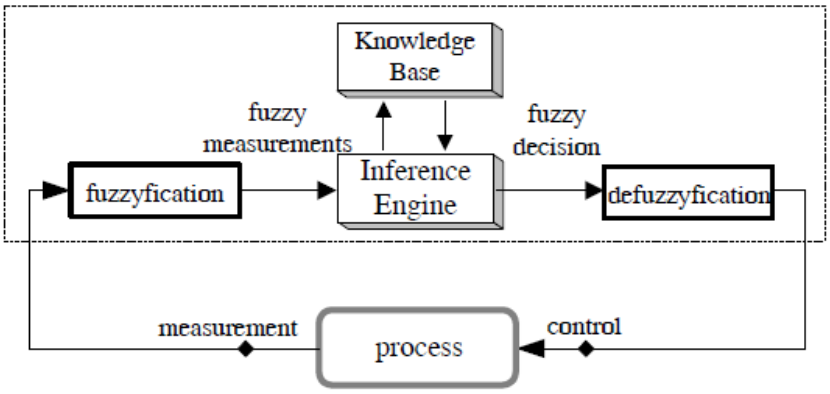

Figure 1.3: Simplified Block Diagram of the Fuzzy Logic Approach

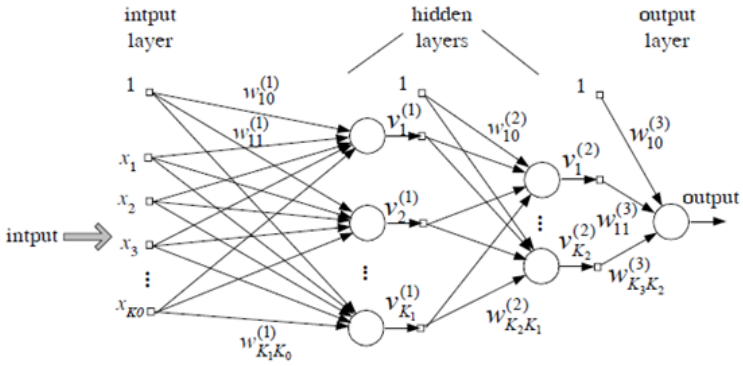

Figure 1.4: Typical Three-Layer Architecture of a Feedforward ANN

The figure 1.4 [7] shows the typical structure of an ANN. The node weights are adjusted as per the given inputs and the required output for each case. We can see that the ANN bases its decision off of previously learned examples. When it comes to fault location, the ANN configuration, the input data and the learning method differ with the type of fault which has to be determined before the fault can be located. For the one end measurement algorithm, the input data consists of the magnitudes of the phase voltages ($|Ui|, \angle Ui$) and currents ($|Ii|, \angle Ii$), magnitudes and phases of incremental positive sequence voltage(s) ($|\Delta Ui|, \angle \Delta Ui$) and current(s) ($|\triangle Ii|, \angle \Delta Ii$) in the phase(s) experiencing the fault, the angles of the phase-phase voltages ($|Uij|, \angle Uij$) and currents ($|Iij|, \angle Iij$), and the magnitudes and angles of the system impedances of the lines ($|Zij|, \angle Zij$).

The figure 1.5 shows the ANN structure used in the estimation of the location of a fault on phase A [7].

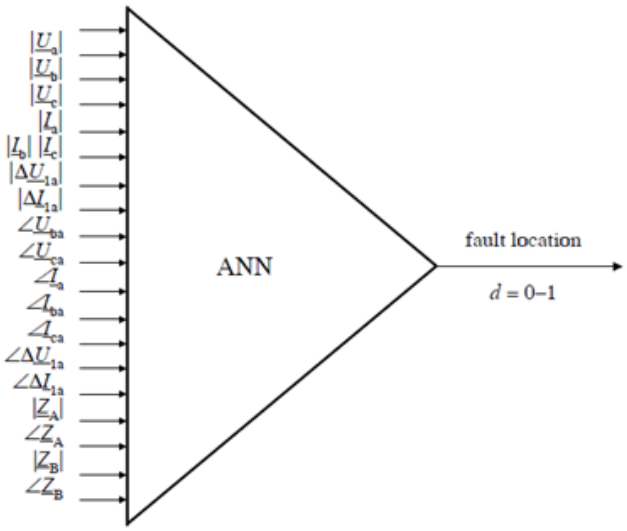

Figure 1.5: ANN Input Structure for Distance to Fault Estimation

AI based techniques require a set of cases to learn the method and to form their set of rules.

Therefore these systems are inaccurate to begin with and get more accurate over time as more and more scenarios are run through them. Since such data might not be readily available, AI based approaches face a hurdle to their implementation.

1.5 Model-based Approach

With the advent of accurate simulation and modelling software it has become easier to create a digital model of the actual feeder/system. These models allow for various scenarios to be tested on the system without actually tampering with the physical system.

In [5] and [9], the authors propose using such a model to facilitate fault location. It is suggested that fault currents be pre-calculated at each section of the feeder by using a short-circuit analysis program on the model of the system available in the simulation software. These pre-calculated fault currents are then compared to the measured fault current on the occurrence of the fault. The match between these two values is then used to locate the fault.

Additional data can be obtained from these models to further improve the fault location. Load allocation and power flow can be performed to accurately determine pre-fault conditions which add further to the accuracy of the fault location technique.

The advantage of this method is that it allows to accurately model the feeder instead of using the simplified model like the impedance based methods do. Also, unlike the AI based methods, this does not require any training and therefore the solutions are accurate from the beginning. The latter is a big hurdle that needs to be overcome since reliable and accurate field data is presently not available readily since not many utilities have PQ monitors at many locations on their feeders.

1.6 Proposed Approach

The aim of this thesis is to formulate a method and create a program that will aid in locating a fault on the system once such an event occurs. The method is based on the approach by Lampley et al. [5]. It is an extension of the model based approach presented above. It involves using the current waveforms available at the substation to determine the location of the fault.

In this thesis, the methodology has been extended to include currents from other locations where PQ monitors are installed. The waveforms are analysed and the most accurate estimate as to the location of the fault is determined.

A program that follows this technique has been implemented and its performance tested on various models of distribution systems. Also, a few tests on field data have been performed.

The technique is modular and can incorporate as many measurements as available in the future.
On the occurrence of a fault, we start off by comparing the measured RMS currents in each phase with their over-current thresholds. This determines the type and the phase(s) of the fault. Once the type of fault is known, the data for the corresponding type of fault is extracted by performing short-circuit analysis on the model of the feeder using the simulation software and the simulated currents are compared with the measured currents to determine the fault location.

Next, the pre and post-fault conditions are used to find the load rejected on each phase. This data is compared with the load flow results for the pre-fault condition to determine the section of the feeder that is now off-line. Also, using the fault current waveform recorded at the measurement device, the time of operation of the protective device is determined. This time is compared to the operating times of all the devices in the system to determine the device that

has operated. These three criteria are used to accurately determine the location of the fault on the system.

1.7 Glossary

Chapter 2 describes the fault location algorithm and the data requirements for its operation. **Chapter 3** explains the modelling of the systems that were used for testing the algorithm based program and the results that were obtained on performing these tests.

The following acronyms have been used throughout this thesis report.

FLA	Fault Location Algorithm
PD	Protection Device
RMS	Root Mean Square
PQ	Real and Reactive Power
SS	Steady State
AP	Allegheny Power, Inc.
ANN	Artificial Neural Network

Chapter 2 The Fault Location Algorithm

This chapter outlines the algorithm that that has been developed to locate a fault. Stated first is a brief explanation of the algorithm which is followed by an in depth description of each module in the algorithm.

2.1 The Algorithm

Figure 2.1 shows the steps involved in the process of fault location. The main algorithm was adopted from [10]. The algorithm can be broken down into three main steps.

Step 1: Calculate the fault current magnitude from the current data that is obtained from the installed PQ monitors on the system.

Step 2: Identify the nodes where the calculated fault current from the model and the measured fault current match. A percentage match of within 3% is considered to account for any inaccuracies in the model.

Step 3: Using the data from the power flow analysis and the duration of the fault determine the protective devices that could have possibly operated. Again, a 3% match is used to account for inaccuracies in the model and to account for measurement and communication errors.

Step 4: Put together the data from the three tests performed to determine the location of the fault and come up with the ideal candidate for the location of the fault on the system. The complete details of the algorithm are given in the following sections where each step is explained in detail.

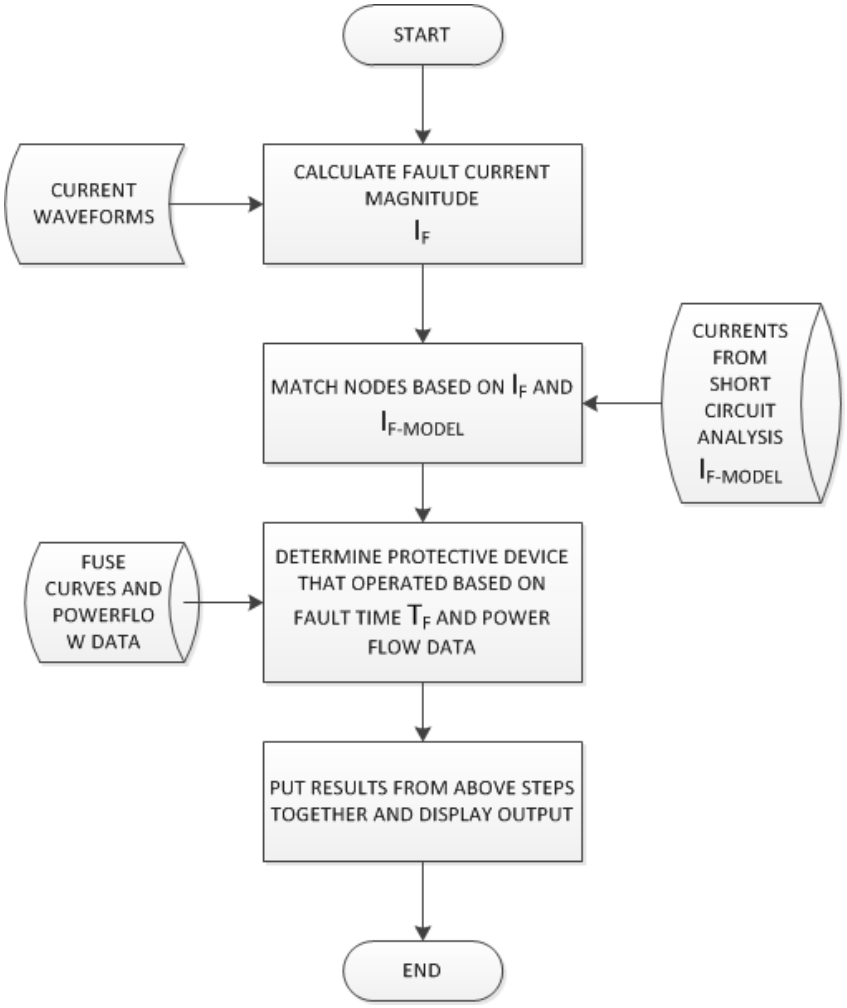

Figure 2.1: Fault Location Algorithm - Flow Chart

Step 1. Calculate Fault Current Parameters

When FLA receives the current waveform from the monitoring device at the substation, the instantaneous waveform is used to obtain the root mean square profile of the fault current. Figure 2.2 shows the typical profile of the instantaneous current on any given phase and the corresponding RMS equivalent waveform. The root mean square waveform is calculated using a moving window of size 1/60 seconds (one cycle of 60 Hz). The measurements are typically sixty-four samples per cycle. Since the grid frequency is 60 Hz, there are sixty-four samples per window

while calculating the root mean square profile. The root mean square profile is calculated for the waveforms for all three phases and the neutral. The neutral current is calculated by summing up the instantaneous currents in the three phases.

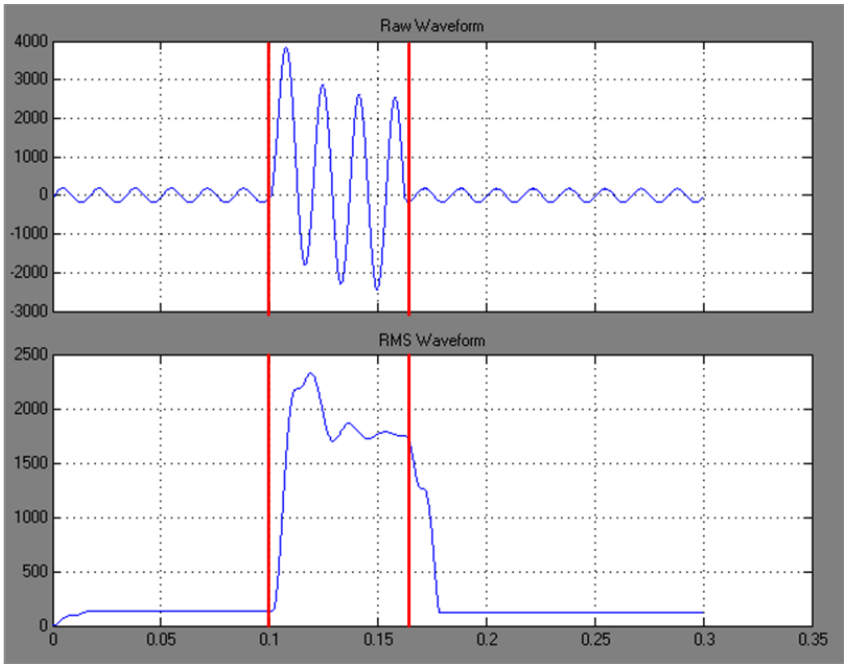

Figure 2.2: Instantaneous and RMS Waveforms

Figure 2.3 shows the important features of the fault current RMS profile. A ground fault is detected if the neutral current is greater than its threshold overcurrent value. The instant of fault inception $T_{inception}$ (Figure 2.3) is determined by finding out the exact cycle when the fault current value $I_F(n)$ becomes greater than the overcurrent threshold. To ensure that the instant is not just one where the currents were oscillating, the condition is checked for two consecutive cycles i.e. during the n^{th} cycle, if

$$I_f(n) < I_{f-Threshold} \;\; \&\& \;\; I_f(n+1) > I_{f-Threshold} \;\; \&\& \;\; I_f(n+2) > I_{f-Threshold} \qquad (2.1)$$

Then the system is said to have experienced a fault. Next the instant at which the protective

device operated, T_{open} (Figure 2.3) is determined using the condition:

$$I_f(n) > I_{f-Threshold} \;\; \&\& \;\; I_f(n+1) < I_{f-Threshold} \;\; \&\& \;\; I_f(n+2) < I_{f-Threshold} \tag{2.2}$$

The difference between the instant of fault inception and the time that the protective operated is the total clearing time.

$$T_{clear} = T_{open} - T_{inception} \tag{2.3}$$

This process is repeated for each phase. Using this data, the time when the fault event occurred is determined.

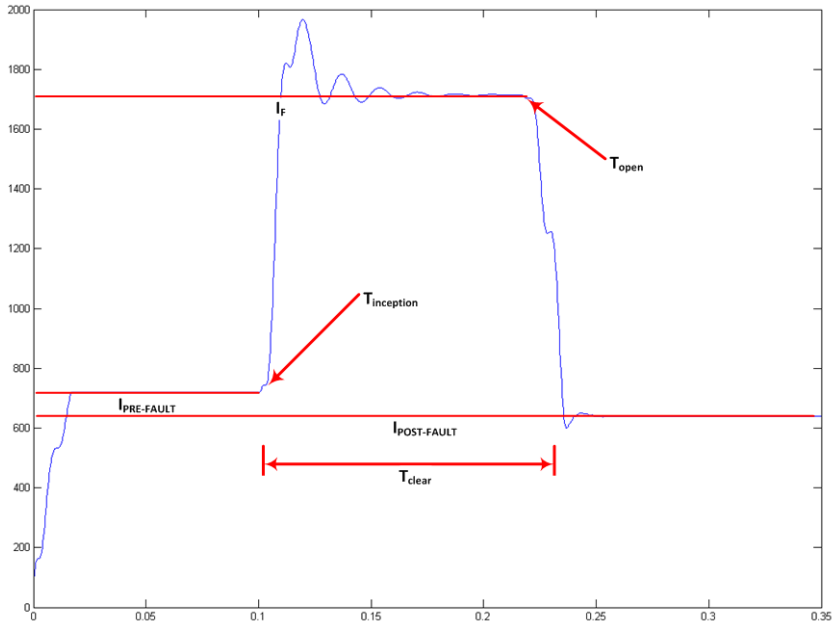

Figure 2.3: Fault Current Waveform

To determine the type and the phase(s) on which the fault occurred, the fault current mag-

nitude from each phase and the neutral is compared to its corresponding overcurrent threshold. These overcurrent thresholds are set for each of the three phases and the neutral. Currents over one and a half times the normal operating range of the system are considered to indicate a fault on a given phase. These values are set to be the overcurrent threshold values. The phase(s) on which the measured currents are greater than their thresholds are said to have experienced a fault. Table 2.1 shows the type of fault for the value of the fault current in each phase.

Table 2.1: Fault Type and Phase(s) Identification Table

Phase A $I_f > I_{f-Threshold}$	Phase B $I_f > I_{f-Threshold}$	Phase C $I_f > I_{f-Threshold}$	Neutral $I_f > I_{f-Threshold}$	*Fault Type*
X	-	-	X	A-G
-	X	-	X	B-G
-	-	X	X	C-G
X	X	-	-	A-B
-	X	X	-	B-C
X	-	X	-	C-A
X	X	X	-	A-B-C

Next the steady state values of the pre-fault, fault and post-fault currents are calculated. For the pre-fault current only the waveform from before the time of fault inception $T_{inception}$ is considered. For the fault current, the waveform from the time of fault inception $T_{inception}$ to fault clearance T_{open} is considered while the post-fault current only takes into account the part of the waveform after the fault has been cleared.

When the fault occurs, the current increases rapidly and oscillates before settling down to a constant value. For the process of fault locating, the value of the current after it settles to its steady state is used. The steady state value of the current I_{f-SS} is calculated using the formula:

If after the n^{th} cycle:

$$\left|\frac{I_f(n+1) - I_f(n)}{I_f(n)}\right| < 0.1 \quad \&\& \quad \left|\frac{I_f(n+2) - I_f(n)}{I_f(n)}\right| < 0.1 \tag{2.4}$$

then

$$I_{f-SS} = \frac{I_f(n+1) + I_f(n)}{I_f(n)} \tag{2.5}$$

Finally, the rejection in load for each phase is calculated as the difference between the pre-fault and post-fault values of the current.

$$I_{rejection} = I_{pre-fault} - I_{post-fault} \tag{2.6}$$

Using the fault current I_{f-SS} a first estimate as to the location of the fault is obtained.

Step 2. Identification of Faulted Nodes

Using the model of the feeder, short circuit analysis is performed using a power system analysis program. This gives the values for the short circuit currents $I_{f-MODEL}$ that would be observed when a fault occurs at each feeder section on the system. In the test system we consider the currents at the substation, and at two other locations where PQ monitors are installed.

The fault current from the measurement device at the substation $I_{f-MEASURED}$ is compared with the fault current values obtained from model up on performing short circuit analysis. Those nodes where the fault currents are found to be within three percent of the actual fault currents are considered as likely candidates for the location of the fault. Also, the nodes are ranked based on the proximity of the values from the model to the measured values of the currents.

$$CurrentError = \frac{I_{f-MEASURED} - I_{f-MODEL}}{I_{f-MODEL}} \tag{2.7}$$

This is done for each of the three phases and for each node. The percentage matches for the all

three currents are averaged and assigned to that node. This data is tabulated and stored.

Step 3. Identification of the Protective Device

Using the time-current characteristics of all the fuses on the feeder, we can find the likely devices that could have isolated the faulted section. This is done in the following way:

1. Using the steady state value of the fault current $I_{f-ACTUAL}$ the time it would have taken for each protective device in the system to operate is calculated from the time-current characteristics of each protective device. From FIGURE 2.4 we see that for the measured value of fault current $I_{f-ACTUAL}$, each fuse has its own operating time.

2. These times are compared with the actual time it took the fault to clear T_{CLEAR}. This data is ranked based on the proximity of T_{TCC} to T_{CLEAR} and ranked as per the formula:

$$TimeError = \frac{T_{TCC} - T_{CLEAR}}{T_{TCC}} \tag{2.8}$$

Next, power flow analysis is performed on the feeder using the most recent loading conditions based on the pre-fault data. From the power flow analysis, the current flow $I_{loadflow}$ through each protective device is determined and tabulated. This data is then used to determine the protective device that operated based on the load rejection at the beginning of the feeder. Once again, the matches are ranked based on the actual load rejection $I_{rejection}$ on each phase.

$$PowerFlowError = \frac{I_{loadflow} - I_{rejection}}{max(I_{loadflow}, I_{rejection})} \tag{2.9}$$

The total power flow error is the average of the power flow errors for all three phases. The power flow error and the time mismatch error are put together and a list of likely protection devices are extracted from this data.

$$NewError = \frac{PowerFLowError + TimeError}{2} \tag{2.10}$$

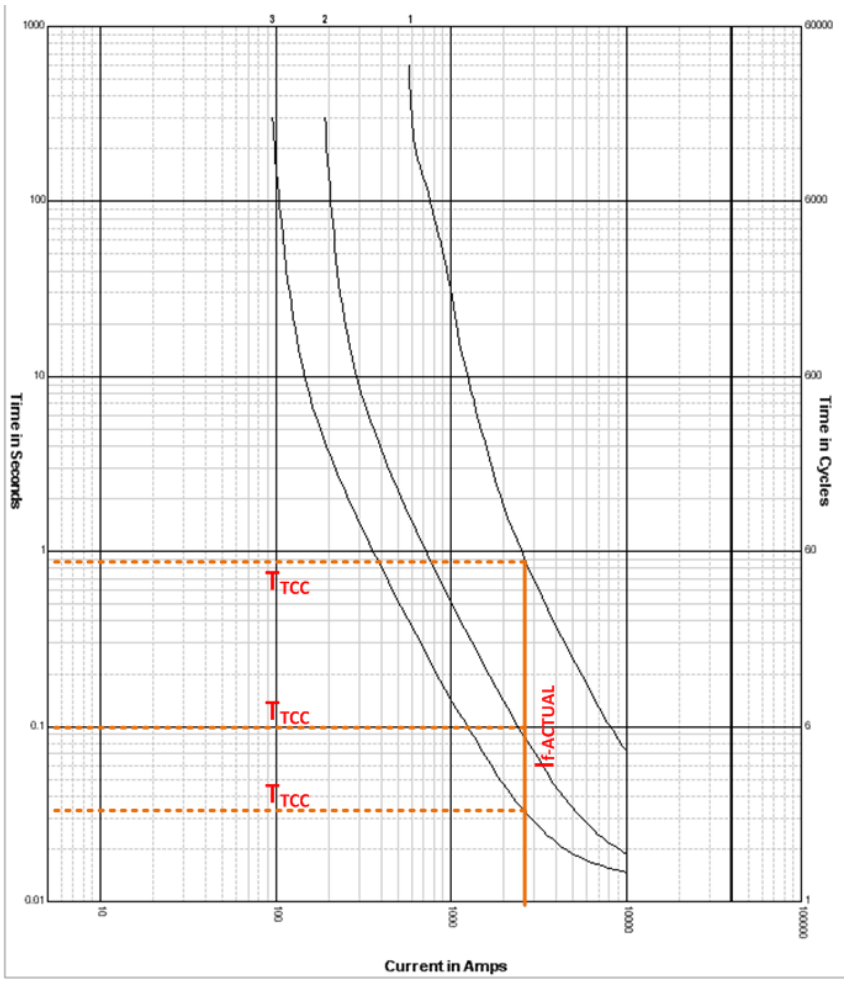

Figure 2.4: TCC Characteristics of Fuses

The complete match for a node is calculated using the formula:

$$CompleteMatch = \frac{max(CurrentError) + max(NewError) - NewError}{max(CurrentError) + max(NewError)} \tag{2.11}$$

Nodes are ranked based on the value of their complete match. The higher the complete match, the more likely the node is to be the location of the fault.

Step 4. Filtering Nodes Based on Additional Measurements

So far, we had only considered the data from the substation viz. the current waveform from the beginning of the feeder. In this study, we consider the use of additional data that is available from the PQ monitors deployed along the feeder at other locations and therefore expand the algorithm to make these calculations more accurate. For example, we have the current waveforms from the switches that have been installed on the feeder. The data from the various monitors has been synchronized so that when a fault occurs at any point on the system, the monitors record the event data irrespective of which monitor actually experienced the event. In this way we have data from multiple sources for the same event.

Firstly, this data is used to reduce the number of nodes based on the fault current data from the simulations for faults at the various nodes i.e. Step 2 is repeated on these waveforms. Then, the list of likely protective devices to have interrupted the fault is reduced based on the data available from the additional current waveforms used by the program. This was done in the following way:

1. If the current from a measurement device is above the fault current threshold it means that the faulted node is downstream of that measurement device.

2. If the current from a measurement device is well below the fault current threshold the fault location is obviously not downstream of the device.

Figure 2.5 shows a distribution feeder with three measurement points M1, M2 and M3. Whenever a fault occurs in the system, M1 measures the fault current. However, based on whether the fault is downstream of points M2 or M3 only one of these devices will measure the fault current. Thus, the nodes downstream of the device that did not measure the fault current can be eliminated from the list of candidate nodes for the location of the fault. This distinction can be made use of to eliminate many nodes if the measurement devices are strategically placed at the various points in the system.

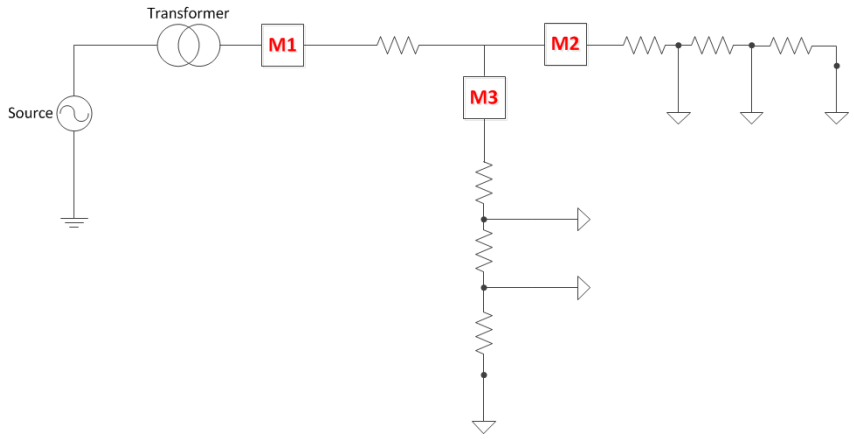

Figure 2.5: Filtering Nodes based on Additional Measurements

At each measurement location, if

$$I_{f-SS} > I_{f-Threshold} \tag{2.12}$$

Then the possible devices to have isolated the fault are downstream of the measurement device. On the other hand, if

$$I_{f-SS} < I_{f-Threshold} \tag{2.13}$$

The device that isolated the fault is upstream of the measurement device. Therefore the list of fuses that would have isolated the fault is reduced thereby reducing the likely candidates for the location of the fault.

Step 5. Output of the Fault Locator

Once the unlikely fuses have been eliminated from the list, the program tries to assemble all the data together to present the output in a way that makes most sense to the user. For this, the program checks under which protective device's zone of protection a possibly faulted node is.

This way it groups all the possible nodes that are protected by the same fuse. This fuse is then assigned a percentage match that is the average of the percentage matches of all the nodes in that device's zone of protection that the program determines to be likely locations for the fault. This information is then output in descending order of percentage match with the most likely device at the top of the list and successive devices having decreasing matches. Each device is followed by the possibly faulted nodes that lie in that device's zone of protection. The program lists only those devices whose percentage matches are more than eighty percent or the top five devices, whichever is higher.

Chapter 3 Performance of the Method

The previous chapter gave an elaborate description of the algorithm used in the program. The next step in the process was to test the effectiveness and the accuracy of the algorithm in determining the locations of the fault once they occurred. This chapter presents the results from these tests. It also outlines the feeders on which these tests were performed and how they were modelled.

To comprehensively test the program two distribution feeders were modeled in MATLAB Simpower. The simulations performed on these systems provided the fault current waveforms that that would be obtained from the actual system. These waveforms are necessary for the fault location program. Faults were simulated on these systems to obtain the fault current waveforms needed by the program to find the location of the faulted node on the feeder.

Feeder 1 was modeled in MATLAB Simpower. The feeder is a reduced version of the actual feeder based on [2]. Feeder 2 was modeled in MATLAB Simpower based on the results of the short circuit analysis performed in DEW on the actual feeder provided by Allegheny Power Inc. These results provided the Thevenin impedance at the point of the fault along with the short circuit currents at these locations. It is a reduced model of the feeder modeled in MATLAB Simpower based on the results from the short circuit analysis performed on the feeder using DEW. This model is used to generate the additional waveforms needed to test the program.

3.1 Feeder 1

This distribution feeder is a reduced model of an actual feeder from [2] and it has 18 nodes. The system is rated at 12kVph-ph. Nodes with both single phase loads as well as three phase loads are present in the system. For the simulations on this feeder, the data for the short circuit

analysis, load flow as well as the current waveforms was obtained from MATLAB Simpower.

3.1.1 Case 1

In this case it is assumed that the feeder is protected by a breaker and 2 reclosers (refer figure 3.1 for the single line diagram of the feeder). Reclosers were two-shot programmed to account for temporary faults. Faults were simulated on this system at various nodes and the corresponding fault current waveforms were input to the program. The fault location program was then executed to determine if the program was able to successfully identify the location of the fault.

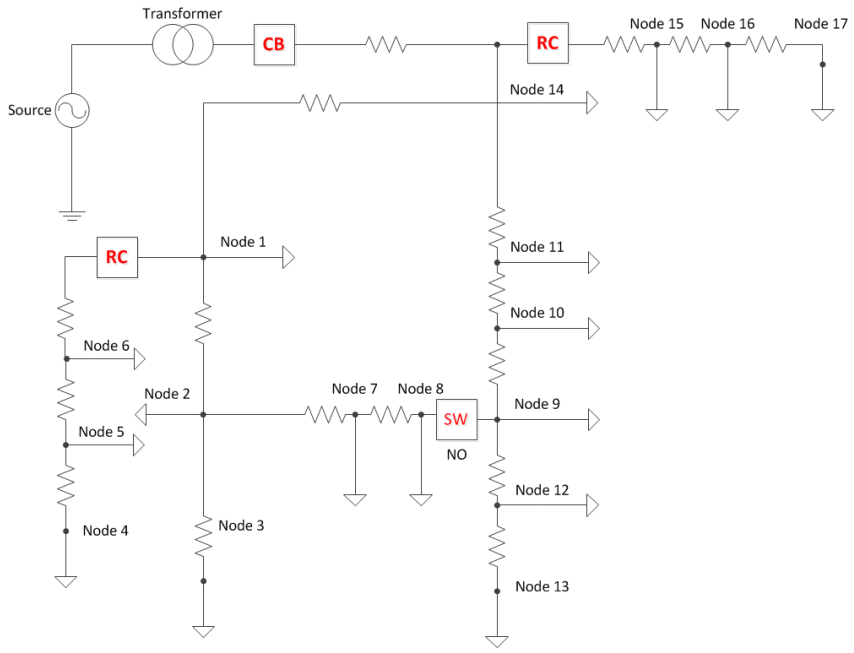

Figure 3.1: Feeder 1 - Case 1 - Single Line Diagram

Single line-ground faults were simulated at the various nodes on the feeder and the data generated (fault current profile seen at the substation end of the feeder) was input to the FLA to see if it was able to accurately locate the fault. Table 3.1 shows the performance of the

program to faults simulated on this system. These test results indicate that even in this small test system, FLA has to choose from multiple candidate locations. In general, FLA localizes the faults quite well with only the data from the substation. However, the localization is not perfect, and there are two cases in which FLA could not identify the correct location. Yellow cells indicate the location was determined correctly. Orange cells indicate that the location was incorrectly determined.

Table 3.1: Test Results for Feeder 1 - Case 1

Faulted Node	**Predicted Nodes**	**Percentage Match**	**Upstream PD**
3	3	98.0033	Substation Breaker
	12	97.4694	Substation Breaker
4	4	83.1314	Recloser B
	12	0.69	Substation Breaker
5	5	83.3306	Recloser B
	6	83.2157	Recloser B
	9	8419	Substation Breaker
	10	1.3457	Substation Breaker
	17	73.9759	Recloser A
6	2	1.5501	Substation Breaker
	6	84.7956	Recloser B
	10	1.2159	Recloser B
	15	74.2036	Substation Breaker
	16	73.8641	Substation Breaker
	17	73.8154	Recloser A
8	8	98.4694	Substation Breaker
	9	98.242	Substation Breaker
9	5	98.3654	Recloser B

Table 3.1 Continued

Faulted Node	Predicted Nodes	Percentage Match	Upstream PD
	9	98.1024	Substation Breaker
	17	0.2976	Substation Breaker
10	2	98.1982	Substation Breaker
	6	46.4291	Recloser B
	10	98.0126	Substation Breaker
	15	0.6654	Recloser A
	16	0.4768	Recloser A
	17	0.4397	Recloser A
11	1	98.4588	Substation Breaker
	11	98.3249	Substation Breaker
12	3	98.0166	Substation Breaker
	4	98.3927	Recloser B
	12	98.1464	Substation Breaker
15	2	1.4077	Substation Breaker
	15	81.6287	Recloser A
	16	81.3939	Recloser A
16	2	0.6323	Substation Breaker
	6	74.4302	Recloser B
	10	1.0198	Substation Breaker
	15	83.3287	Recloser A
	16	83.5571	Recloser A
17	5	73.3879	Recloser B
	6	73.3707	Recloser B
	9	0.6694	Substation Breaker
	10	1.2687	Substation Breaker

Table 3.1 Continued

Faulted Node	Predicted Nodes	Percentage Match	Upstream PD
	17	82.4438	Recloser A

Analysing the results from these tests, it was determined that FLA was unable to accurately determine the fault location for four cases out of the twelve. This inability can be attributed to one main reason. The program operates by using both the fault current as well as the pre and post event currents. When the number of protective devices is low, the load rejection is the same for all of the devices under each device's zone of protection. Therefore in this case, as there are only three protective devices, the program has a hard time accurately pinpointing the fault location.

Summary: Number of cases – 12

Success – 8

Failure – 4

For the cases where the program was unable to correctly identify the fault location, we find that the accurate location was very close to what was predicted by the program. In fact, it is the second highest in every case where the location is incorrect. Also, the difference between the correct location and the determined location is less than 0.5 percent.

3.1.2 Case 2

This model is a modification over Case 1. Here, all the reclosers were removed and the system was protected by six fuses.

These fuses were placed along each lateral on the feeder. Figure 3.2 shows the single line diagram for this feeder configuration. The exact Matlab model can be found in the appendix.

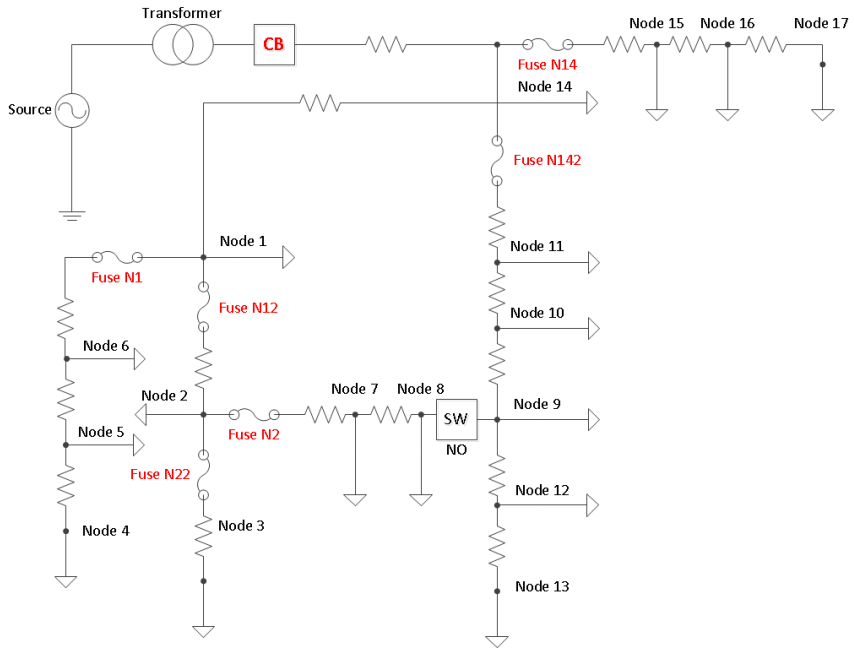

Figure 3.2: Feeder 1 - Case 2 - Single Line Diagram

Once again, faults were simulated throughout the system. The resulting current waveforms were input to the fault location program to find out if the program located the fault successfully. Table 3.2 shows the results of these tests. The table shows the nodes predicted by the program for a fault at a given location and also the associated protective device that could have operated. Again, yellow cells indicate that the program identified the location correctly, whereas the orange cells show those cases where the program had difficulties in deducing the fault location.

Table 3.2: Test Results for Feeder 1 - Case 2

Faulted Node	**Predicted Nodes**	**Percentage Match**	**Upstream PD**
3	3	95.775	N22
	12	0.123	N142
4	4	85.437	N1
	12	76.371	N142
5	5	84.8	N1

Table 3.2 Continued

Faulted Node	Predicted Nodes	Percentage Match	Upstream PD
	6	84.678	N1
	9	76.601	N142
	10	77.175	N142
	17	95.366	N14
6	2	80.112	N12
	5	85.199	N1
	6	85.246	N1
	7	0.28	N2
	10	93.473	N142
	16	75.153	N14
	17	75.074	N14
8	5	1.101	N1
	8	94.1	N2
	9	0.603	N142
	17	1.581	N14
9	5	94.2351	N1
	8	0.2103	N2
	9	95.7803	N142
	17	83.8772	N14
10	2	88.944	N12
	6	94.1092	N1
	7	0.5467	N2
	10	95.3565	N142
	15	83.8163	N14

Table 3.2 Continued

Faulted Node	Predicted Nodes	Percentage Match	Upstream PD
	16	83.6726	N14
11	1	93.5193	Substation Breaker
	11	94.7619	N142
12	3	44.2308	N22
	4	94.8699	N1
	12	96.1493	N142
15	2	37.275	N12
	7	4.371	N2
	10	24.52	N142
	15	43.374	N14
	16	42.707	N14
16	2	39.558	N12
	6	35.587	N1
	7	1.855	N2
	10	26.16	N142
	15	45.362	N14
	16	46.009	N14
17	5	35.967	N1
	6	35.657	N1
	9	29.497	N142
	10	28.947	N142
	17	47.918	N14

From the results it is observed that the program correctly recognizes location of the fault for

almost all cases. The program got the location wrong for just one case. This is due to the fact that both fault currents are similar and therefore their operating times are the same on account of the fuses being the same type.

Summary: Number of cases	–	**12**
Success	–	**11**
Failure	–	**1**

When compared to the precious case, it is observed that the number of incorrect determinations has gone down. This is attributed to the fact that there are now more protection devices on the system and the program thus has more power flow data to base its calculations on.

The figure 3.3 shows the nodes predicted by the program for a fault at Node 15. As can be seen, apart from Node 16 the rest of the nodes all fall under different zones of protection. Node 15 and 16 are very close to each other and therefore the program determines both to be likely locations for the fault as they have similar fault currents and they fall under the same protective devices zone of protection. The prediction for nodes 2 and 7 is based solely on the fact that the short circuit currents are comparable to the current at Node 15 i.e. Current Error is small. However they do not fit the other criteria Time Error and Power Flow Error are large and therefore, it is observed that their percentage matches are low in spite of them being identified as possible fault locations.

3.2 Feeder 2

One of the actual feeders from Allegheny Power (AP) has been used to further test the program. Short circuit analysis and load flow studies were performed on this feeder model using DEW. The fault current to be seen at the substation end of the circuit was simulated using MATLAB Simulink. These data were then input to the program to see its accuracy with fault location.

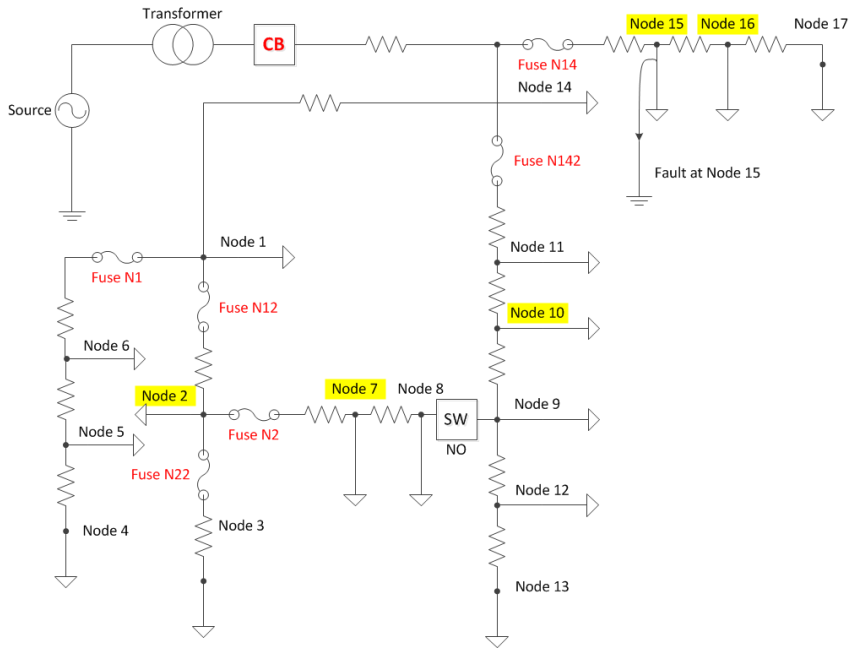

Figure 3.3: Fault at Node 15

Using the model of the actual system provided by Allegheny Power Inc., equivalent systems were modeled in MATLAB Simulink using the Thevenin equivalent impedances of the lines and the laterals and the voltages calculated from the short circuit analysis on the feeder using DEW. These models provided the waveforms for faults that were simulated at particular nodes. This waveform was used to locate the faults using the fault location program. Figure 3.4 shows the single line diagram for this system. The exact model for the system can be found in the appendix.

Out of the total of 433 nodes on the feeder, the program was tested for faults simulated on models created for 5 nodes in the feeder. Table 3.3 shows the results obtained by the program for these fault simulations.

Table 3.3: Test Results for Feeder 2

Faulted Node	**Predicted Nodes**	**Percentage Match**	**Upstream PD**
2A4990	2A4990	84.049	FUSE654421560

Table 3.3 Continued

Faulted Node	Predicted Nodes	Percentage Match	Upstream PD
	1W0136	70.228	FUSE654421454
1002850	P4538	85.401	FUSE654427667
	P4539		
	P4463	86.976	FUSE654427653
	P4489		
	P4408	95.639	FUSE1132303995
	P4412		
	P4416		
	P4417		
	P4420		
	P4110		
	P4109		
	1002850		
	P4405	88.751	RECLOSER
	P4401		
	P4400		
	P4398		
	P4396		
	P4393		
	P4392		
	P4384		
	P4391		
	P4383		
	P4607	86.442	FUSE654421506
	P4609		

Table 3.3 Continued

Faulted Node	Predicted Nodes	Percentage Match	Upstream PD
	R0711		
	R0712		
	P4614		
1254532	2A7744	86.879	
	P4624	70.767	RECLOSER
	P4592		
	P4591		
	P4585		
	P4580		
	P4579		
	P4594		
	2A7818	84.794	FUSE654421534
	2A7819		
	2A7820		
	P4582		
	1248612		
	P4597	85.758	FUSE654421506
	1248664	88.792	FUSE1026772775
	1248663		
	1254860		
	2050951		
	2050952		
	1130074		
	1254532		
	1254531		

Table 3.3 Continued

Faulted Node	Predicted Nodes	Percentage Match	Upstream PD
	2050966		
	1254530		
	1254528		
	1254859		
	2050943		
	2050963		
	1254539		
1254804	P4502	86.347	FUSE654427653
	P4508		
	P4509		
	P4513		
	P4378	99.532	RECLOSER
	P4375		
	P4238		
	P4236		
	N7970		
	N7955		
	1063586		
	N7972		
	N7973		
	P4240		
	P4247		
	1254804	99.698	FUSE1052482746
	P4266		
	P4268		

Table 3.3 Continued

Faulted Node	Predicted Nodes	Percentage Match	Upstream PD
	1267645		
	1254806	71.082	FUSE1052482716
	1254807		
	1254809		
	P4616	86.364	FUSE1132303995
	P4618	86.362	FUSE654421506
P4622	P4515	89.636	FUSE654427653
	P4520		
	P4522		
	P4619	90.913	FUSE654421506
	P4622		
2A7818	1254860	83.899	FUSE1026772775
	2050951		
	2050952		
	1130074		
	1254532		
	1254533		
	1254531		
	2051112		
	2050966		
	1254530		
	1254528		
	1254859		
	2050943		
	2050963		

Table 3.3 Continued

Faulted Node	Predicted Nodes	Percentage Match	Upstream PD
	1254539		
	1W0136	71.0325	FUSE654421454
	2A7744	85.5116	FUSE654421480
	P4597	86.3038	FUSE654421506
	P4602		
	2A7818	88.3566	FUSE654421534
	2A7819		
	2A7820		
	1248612		
	P4582		
	2A4990	70.6921	FUSE654421560
	P4591	69.5617	RECLOSER
	P4585		
	P4580		
	P4579		
	P4577		
	P4574		
	P4535		
	P4594		
P4459	P4406	81.6887	FUSE1132303995
	P4408		
	P4412		
	P4416		
	P4417		
	P4459	85.2459	FUSE654421493

Table 3.3 Continued

Faulted Node	Predicted Nodes	Percentage Match	Upstream PD
	P4582	88.4043	FUSE654421506
	P4602		
	1E8327		
	P4605		
	P4607		
	P4609		
	P4461	88.5782	FUSE654427653
	P4463		
	P4536	85.3777	FUSE654427667
	P4538		
	P4539		
	P4577	71.8238	RECLOSER
	P4574		
	P4535		
	P4458		
	P4457		
	P4453		
	2A7715		
	P4451		
	P4405		
	P4401		
	P4400		
	P4398		
P4597	1248664	85.3589	FUSE1026772775
	1254860		

Table 3.3 Continued

Faulted Node	Predicted Nodes	Percentage Match	Upstream PD
	2050951		
	2050952		
	1130074		
	1254532		
	1254533		
	1254531		
	2051112		
	2050966		
	1254530		
	1254528		
	1254859		
	2050943		
	2050963		
	1254539		
	2A7744	87.1964	FUSE654421480
	P4597	88.2458	FUSE654421506
	P4602		
	2A7818	87.1078	FUSE654421534
	2A7819		
	2A7820		
	1248612		
	P4582		
	2A4990	68.57	FUSE654421560
	P4585	70.0586	RECLOSER
	P4580		

Table 3.3 Continued

Faulted Node	Predicted Nodes	Percentage Match	Upstream PD
1254806	1254806	80.156	FUSE1052482716
	1254807		
	1254809		
	1254804	57.3359	FUSE1052482746
	P4266		
	P4268		
	1267645		
	N7977	7.9506	FUSE1071439054
	1279017	46.2591	FUSE1146924279
	P4616	64.3954	FUSE654421506
	P4618		
	P4619		
	P4496	45.8701	FUSE654421586
	P4498		
	P4241	43.048	FUSE654427484
	N7974	46.2295	FUSE654427566
	N7976		
	P4509	63.4096	FUSE654427653
	P4513		
	P4515		
	P4236	48.8939	RECLOSER
	P4235		
	N7970		
	N7955		
	1063586		

Table 3.3 Continued

Faulted Node	Predicted Nodes	Percentage Match	Upstream PD
	N7972		
	N7973		
	P4247		
2C0234	1076088	53.4846	FUSE654421097
	N7094	57.0198	FUSE654421142
	1077826		
	1089765		
	2B4053	57.1774	FUSE654421166
	2C0234		
	N7097	5.394	RECLOSER
	N7100		

Summary: Number of cases – **10**

Success – **9**

Failure – **1**

As can be seen from the results, for almost all the cases the program was able to localize the fault. However in some cases the program cannot pinpoint the location. This happens in cases where there are quite a few small branches supplied from a lateral (refer figure 3.5), and thus all these small sub-laterals are electrically the same distance from the substation, i.e. they create the same fault current profile. Also due to the similarity between the various loads and fuses, the program predicts a large number of nodes to be the likely locations for the fault. Nevertheless, since these candidate nodes are quite close to each other physically, FLA identifies the correct fuse which has blown due to fault, and hence this information will be quite helpful in the actual

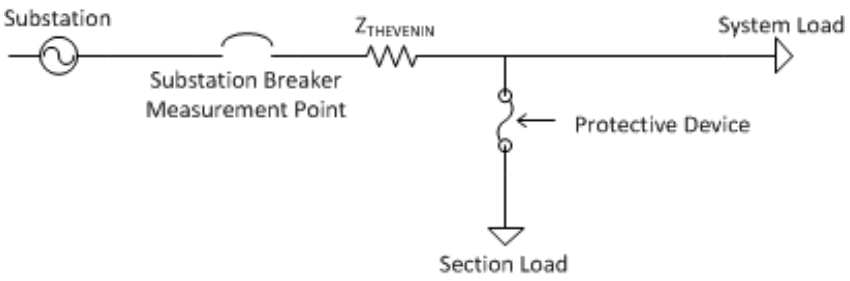

Figure 3.4: Feeder 2 - Equivalent Model

pinpointing of the fault on the field by the repair crew.

From the results so far, we see that FLA gives a lot of candidate nodes for a fault. Though, it localized the faulted location accurately, there was still a lot of data to parse through before the faulted node was accurately identified. Also it is almost impossible to determine which node under a particular protective device experienced the fault. However it is possible to determine the protective device that operated to isolate the fault.

Each fuse protects multiple nodes. Usually, the results obtained from short circuit analysis for these nodes are very close to each other. Therefore when any of these nodes experiences a fault, it is very difficult to accurately pinpoint which particular node is faulted. However, it is possible to determine which fuse interrupted the fault current; and that is exactly what the program set out to achieve.

Therefore, the program was modified to show the protective device that would most likely have operated to isolate the fault.

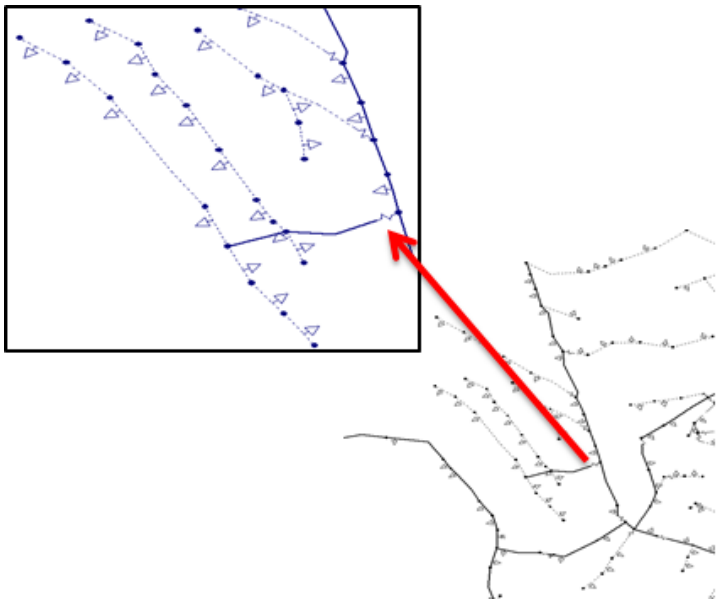

Figure 3.5: Zone of Protection for a Fuse

3.3 FLA with Additional Field Monitors

The use of only one monitoring device to obtain the measurements from the entire system meant that the program showed multiple possibilities for the location of the fault in different zones of protection within the distribution system. These locations were determined based on the values of fault current at these points so it was obvious that multiple locations would crop up since the lines split up at various points and therefore there would exist multiple laterals with the same fault currents from the point of measurement.

To eliminate some of these nodes it was necessary to include additional measurements so that the program had more data to base its calculations up on. Therefore the trip status of a few protective devices present in the system was included in the data that was input to the program. With the inclusion of the trip status of these devices it was possible to pinpoint the exact protection zone in which the fault had taken place and thereby eliminate some of the nodes (which basic FLA showed as possible fault locations) that were present in other protection zones.

To test the impact of having additional data, two fuses on the Feeder 1 model, Fuses N1 and N142, were assumed to be monitored and when they saw a fault they relayed that information back to the FLA. Table 3.4 shows the results for this simulated case. As the table shows, the addition of these measurements dramatically reduced the set of possible fault locations as this new data helped pinpoint the protection zone with a higher degree of accuracy.

Table 3.4: Impact of Additional Measurements on Feeder 1

	Possible Nodes	
Faulted Node	**Basic FLA**	**FLA - Additional Measurements**
3	3	3
	12	
4	4	4
	12	
5	5	5
	6	6
	9	
	10	
	17	
6	2	5
	5	6
	6	
	7	
	10	
	16	
	17	
8	5	8
	8	17

Table 3.4 Continued

	Possible Nodes	
Faulted Node	**Basic FLA**	**FLA - Additional Measurements**
	9	
	17	
9	5	9
	8	
	9	
	17	
10	2	10
	6	
	7	
	10	
	15	
	16	
11	1	11
	11	
12	3	12
	4	
	12	
15	2	2
	7	7
	10	15
	15	16
	16	
16	2	2
	6	7

Table 3.4 Continued

	Possible Nodes	
Faulted Node	**Basic FLA**	**FLA - Additional Measurements**
	7	15
	10	16
	15	
	16	
17	5	17
	6	
	9	
	10	
	17	

From the results we see that for the worst cases, the addition of measurements from additional devices reduces the list of candidate locations quite well. In fact, for the case with the maximum possibilities (Fault @ Node 6), the additional measurements reduce the list to just two and both of these nodes fall in the same protection zone (Nodes 5 and 6).

In the case of the fault at node 5, FLA with just one measurement gets the location wrong (Node 17). However, when the additional measurements are incorporated, the program eliminated the wrong node as it had a measurement which said that the device protecting the wrongly identified node (Fuse N14) had not operated and therefore could not be the fault location. Thus the program eliminated unlikely fault locations thereby arriving at the right choice for the location of the fault.

Summary: Number of cases – 12

Success	–	**12**
Failure	–	**0**

To illustrate effect of additional data on Feeder 2, one fuse on the feeder **FUSE1026772775** is monitored. This is the fuse with the largest number of downstream nodes. Table 3.5 shows the comparison of the results from Basic FLA and the results obtained by including this additional measurement from the fuse.

As the table indicates, the addition of even one monitoring device helps reduce the candidate locations quite a bit. The highlighted cells are the locations provided by the program.

Table 3.5: Test Results on Feeder 2 with Two Monitoring Points

	Basic FLA				Additional Measurements			
Faulted Node	**Predicted Nodes**	**Match**	**Upstream PD**	**PD Match**	**Predicted Nodes**	**Match**	**Upstream PD**	**PD Match**
2A4990	2A4990	84.05	FUSE654421560	84.05	2A4990	84.05	FUSE654421560	84.05
	1W0136	70.23	FUSE654421454	70.23	1W0136	70.23	FUSE654421454	70.23
1002850	P4538	85.33	FUSE654427667	85.37	P4538	85.33	FUSE654427667	85.37
	P4539	85.4			P4539	85.4		
	P4463	86.98	FUSE654427653	87.06	P4463	86.98	FUSE654427653	87.06
	P4489	87.14			P4489	87.14		
	P4408	95.51	FUSE1132303995	95.59	P4408	95.51	FUSE1132303995	95.59
	P4412	95.55			P4412	95.55		
	P4416	95.62			P4416	95.62		
	P4417	95.66			P4417	95.66		
	P4420	95.61			P4420	95.61		
	P4110	95.58			P4110	95.58		
	P4109	95.53			P4109	95.53		

Table 3.5 Continued

	Basic FLA				Additional Measurements			
Faulted Node	**Predicted Nodes**	**Match**	**Upstream PD**	**PD Match**	**Predicted Nodes**	**Match**	**Upstream PD**	**PD Match**
	1002850	95.64			1002850	95.64		
	P4405	88.75	RECLOSER	88.82				
	P4401	88.79						
	P4400	88.83						
	P4398	88.86						
	P4396	88.89						
	P4393	88.88						
	P4392	88.87						
	P4384	88.8						
	P4391	88.8						
	P4383	88.74						
	P4607	86.44	FUSE654421506	86.51	P4607	86.44	FUSE654421506	86.51
	P4609	86.52			P4609	86.52		
	R0711	86.59			R0711	86.59		

Table 3.5 Continued

	Basic FLA				Additional Measurements			
Faulted Node	**Predicted Nodes**	**Match**	**Upstream PD**	**PD Match**	**Predicted Nodes**	**Match**	**Upstream PD**	**PD Match**
	R0712	86.5			R0712	86.5		
	P4614	86.5			P4614	86.5		
1254532	2A7744	86.75	FUSE654421480					
	P4624	70.42	RECLOSER	70.59				
	P4592	70.52						
	P4591	70.62						
	P4585	70.77						
	P4580	70.64						
	P4579	70.53						
	P4594	70.67						
	2A7818	84.79	FUSE654421534	84.61				
	2A7819	84.72						
	2A7820	84.57						
	P4582	84.48						

Table 3.5 Continued

	Basic FLA				Additional Measurements			
Faulted Node	**Predicted Nodes**	**Match**	**Upstream PD**	**PD Match**	**Predicted Nodes**	**Match**	**Upstream PD**	**PD Match**
	1248612	84.47						
	P4597	85.76	FUSE654421506					
	1248664	88.48	FUSE1026772775	88.66	1248664	88.48	FUSE1026772775	88.66
	1248663	88.41			1248663	88.41		
	1254860	88.59			1254860	88.59		
	2050951	88.7			2050951	88.7		
	2050952	88.86			2050952	88.86		
	1130074	88.73			1130074	88.73		
	1254532	88.79			1254532	88.79		
	1254531	88.72			1254531	88.72		
	2050966	88.55			2050966	88.55		
	1254530	88.58			1254530	88.58		
	1254528	88.54			1254528	88.54		
	1254859	88.41			1254859	88.41		

Table 3.5 Continued

	Basic FLA				Additional Measurements			
Faulted Node	**Predicted Nodes**	**Match**	**Upstream PD**	**PD Match**	**Predicted Nodes**	**Match**	**Upstream PD**	**PD Match**
	2050943	88.84			2050943	88.84		
	2050952	88.85			2050952	88.85		
	2050963	88.79			2050963	88.79		
	1254539	88.69			1254539	88.69		
1254804	P4502	86.35	FUSE654427653	86.35	P4502	86.35	FUSE654427653	86.35
	P4508	86.35			P4508	86.35		
	P4509	86.36			P4509	86.36		
	P4513	86.35			P4513	86.35		
	P4378	99.52	RECLOSER	99.53				
	P4375	99.52						
	P4238	99.53						
	P4236	99.53						
	P4235	99.53						
	N7970	99.53						

Table 3.5 Continued

	Basic FLA				Additional Measurements			
Faulted Node	**Predicted Nodes**	**Match**	**Upstream PD**	**PD Match**	**Predicted Nodes**	**Match**	**Upstream PD**	**PD Match**
	N7955	99.53						
	1063586	99.53						
	N7972	99.53						
	N7973	99.53						
	P4240	99.53						
	P4247	99.53						
	1254804	99.7	FUSE1052482746	99.7	1254804	99.7	FUSE1052482746	99.7
	P4266	99.7			P4266	99.7		
	P4268	99.69			P4268	99.69		
	1267645	99.69			1267645	99.69		
	1254806	71.08	FUSE1052482716	71.08	1254806	71.08	FUSE1052482716	71.08
	1254807	71.08			1254807	71.08		
	1254809	71.08			1254809	71.08		
	P4616	86.36	FUSE1132303995	86.36	P4616	86.36	FUSE1132303995	86.36

Table 3.5 Continued

	Basic FLA				Additional Measurements			
Faulted Node	**Predicted Nodes**	**Match**	**Upstream PD**	**PD Match**	**Predicted Nodes**	**Match**	**Upstream PD**	**PD Match**
	P4618	86.36	FUSE654421506	86.36	P4618	86.36	FUSE654421506	86.36
P4622	P4515	89.55	FUSE654427653	89.64	P4515	89.55	FUSE654427653	89.64
	P4520	89.73			P4520	89.73		
	P4522	89.64			P4522	89.64		
	P4619	90.77	FUSE654421506	90.84	P4619	90.77	FUSE654421506	90.84
	P4622	90.91			P4622	90.91		
2A7818	1254860	84.35	FUSE1026772775	84.06				
	2050951	84.5						
	2050952	84.62						
	1130074	76.01						
	1254532	84.72						
	1254533	84.74						
	1254531	84.78						
	2051112	84.8						

Table 3.5 Continued

	Basic FLA				Additional Measurements			
Faulted Node	**Predicted Nodes**	**Match**	**Upstream PD**	**PD Match**	**Predicted Nodes**	**Match**	**Upstream PD**	**PD Match**
	2050966	84.69						
	1254530	84.72						
	1254528	84.68						
	1254859	84.55						
	2050943	84.7						
	2050963	84.55						
	1254539	84.46						
	1W0136	71.0325	FUSE654421454	71.0325	1W0136	71.03251	FUSE654421454	71.03251
	2A7744	85.5116	FUSE654421480	85.5116	2A7744	85.51159	FUSE654421480	85.51159
	P4597	86.3585	FUSE654421506	86.2764	P4597	86.3585	FUSE654421506	86.27635
	P4602	86.1942			P4602	86.1942		
	2A7818	88.2716	FUSE654421534	88.3547	2A7818	88.2716	FUSE654421534	88.354696
	2A7819	88.3969			2A7819	88.39685		
	2A7820	88.4584			2A7820	88.4584		

Table 3.5 Continued

	Basic FLA				Additional Measurements			
Faulted Node	**Predicted Nodes**	**Match**	**Upstream PD**	**PD Match**	**Predicted Nodes**	**Match**	**Upstream PD**	**PD Match**
	1248612	88.3659			1248612	88.36593		
	P4582	88.2807			P4582	88.2807		
	2A4990	69.4981	FUSE654421560	69.4981	2A4990	69.4981	FUSE654421560	69.4981
	P4591	69.4467	RECLOSER	69.5641				
	P4585	69.6669						
	P4580	69.8454						
	P4579	69.6973						
	P4577	69.5087						
	P4574	69.4559						
	P4535	69.3933						
	P4594	69.4989						
P4459	P4582	86.6871	FUSE654421547	86.6871	P4582	86.6871	FUSE654421547	86.6871
	P4577	71.6359	RECLOSER	71.8106				
	P4574	71.6812						

Table 3.5 Continued

	Basic FLA				Additional Measurements			
Faulted Node	**Predicted Nodes**	**Match**	**Upstream PD**	**PD Match**	**Predicted Nodes**	**Match**	**Upstream PD**	**PD Match**
	P4535	71.8152						
	P4458	71.7686						
	P4457	71.8106						
	P4453	71.8528						
	2A7715	71.8782						
	P4451	71.8995						
	P4405	72.0169						
	P4401	71.877						
	P4400	71.787						
	P4398	71.7049						
	P4536	85.4879	FUSE654427667	85.3777	P4536	85.48789	FUSE654427667	85.37773
	P4538	85.4123			P4538	85.41231		
	P4539	85.233			P4539	85.23299		
	P4459	85.2459	FUSE654421493	85.2459	P4459	85.2459	FUSE654421493	85.2459

Table 3.5 Continued

	Basic FLA				Additional Measurements			
Faulted Node	**Predicted Nodes**	**Match**	**Upstream PD**	**PD Match**	**Predicted Nodes**	**Match**	**Upstream PD**	**PD Match**
	P4461	88.5383	FUSE654427653	88.5982	P4461	88.5383	FUSE654427653	88.598185
	P4463	88.6581			P4463	88.65807		
	P4406	81.2812	FUSE1132303995	81.1547	P4406	81.2812	FUSE1132303995	81.154694
	P4408	81.339			P4408	81.339		
	P4412	81.1812			P4412	81.1812		
	P4416	81.032			P4416	81.032		
	P4417	80.9401			P4417	80.94007		
	P4602	88.4951	FUSE654421506	88.6975	P4602	88.4951	FUSE654421506	88.697544
	1E8327	88.6361			1E8327	88.63614		
	P4605	88.8057			P4605	88.80569		
	P4607	88.8957			P4607	88.89569		
	P4609	88.6551			P4609	88.6551		
P4597	2A7744	87.1964	FUSE654421480	87.1964	2A7744	87.1964	FUSE654421480	87.1964
	P4585	70.0035	RECLOSER	70.0586				

Table 3.5 Continued

	Basic FLA				Additional Measurements			
Faulted Node	**Predicted Nodes**	**Match**	**Upstream PD**	**PD Match**	**Predicted Nodes**	**Match**	**Upstream PD**	**PD Match**
	P4585	70.1466						
	P4580	70.0257						
	2A7818	87.152	FUSE654421534	87.115	2A7818	87.152	FUSE654421534	87.114988
	2A7819	87.2663			2A7819	87.26627		
	2A7820	87.111			2A7820	87.11096		
	1248612	87.0182			1248612	87.01819		
	P4582	87.0275			P4582	87.02752		
	2A4990	68.57	FUSE654421560	68.57	2A4990	68.57	FUSE654421560	68.57
	P4597	88.3447	FUSE654421506	88.1964	P4597	88.3447	FUSE654421506	88.19641
	P4602	88.0481			P4602	88.04812		
	1248664	85.0512	FUSE1026772775	85.3277				
	1254860	85.163						
	2050951	85.3116						
	2050952	85.4314						

Table 3.5 Continued

	Basic FLA				Additional Measurements			
Faulted Node	**Predicted Nodes**	**Match**	**Upstream PD**	**PD Match**	**Predicted Nodes**	**Match**	**Upstream PD**	**PD Match**
	1130074	85.4511						
	1254532	85.4882						
	1254533	85.4693						
	1254531	85.4145						
	2051112	85.3871						
	2050966	85.2762						
	1254530	85.304						
	1254528	85.2669						
	1254859	85.1353						
	2050943	85.4615						
	2050963	85.3646						
	1254539	85.2675						
1254806	P4496	45.5653	FUSE654421586	45.7939	P4496	45.56529	FUSE654421586	45.793895
	P4498	46.0225			P4498	46.0225		

Table 3.5 Continued

	Basic FLA				Additional Measurements			
Faulted Node	**Predicted Nodes**	**Match**	**Upstream PD**	**PD Match**	**Predicted Nodes**	**Match**	**Upstream PD**	**PD Match**
	P4509	63.228	FUSE654427653	63.4096	P4509	63.228	FUSE654427653	63.40956667
	P4513	63.6354			P4513	63.6354		
	P4515	63.3653			P4515	63.3653		
	1279017	46.2591	FUSE1146924279	46.2591	1279017	46.2591	FUSE1146924279	46.2591
	P4236	48.6493	RECLOSER	48.8894				
	P4235	48.674						
	N7970	48.848						
	N7955	48.9881						
	1063586	48.9149						
	N7972	49.0076						
	N7973	49.1349						
	P4247	48.8981						
	N7974	46.241	FUSE654427566	46.2295	N7974	46.241	FUSE654427566	46.2295
	N7976	46.218			N7976	46.218		

Table 3.5 Continued

	Basic FLA				Additional Measurements			
Faulted Node	**Predicted Nodes**	**Match**	**Upstream PD**	**PD Match**	**Predicted Nodes**	**Match**	**Upstream PD**	**PD Match**
	P4241	43.048	FUSE654427484	43.048	P4241	43.04801	FUSE654427484	43.04801
	1254804	57.2232	FUSE1052482746	67.1388	1254804	57.2232	FUSE1052482746	67.13879286
	P4266	57.274			P4266	57.27396		
	1254806	80.2803			1254806	80.2803		
	1254807	80.1259			1254807	80.12593		
	1254809	80.1089			1254809	80.1089		
	P4268	57.4796			P4268	57.47964		
	1267645	57.4796			1267645	57.47964		
	P4616	64.2103	FUSE654421506	64.3954	P4616	64.21027	FUSE654421506	64.39538667
	P4618	64.755			P4618	64.75504		
	P4619	64.2209			P4619	64.22085		
2C0234	1076088	53.4846	FUSE654421097	53.4846	1076088	53.4846	FUSE654421097	53.4846
	N7094	56.6031	FUSE654421142	56.9347	N7094	56.60314	FUSE654421142	56.93466333
	1077826	56.9257			1077826	56.92565		

Table 3.5 Continued

	Basic FLA				Additional Measurements			
Faulted Node	**Predicted Nodes**	**Match**	**Upstream PD**	**PD Match**	**Predicted Nodes**	**Match**	**Upstream PD**	**PD Match**
	1089765	57.2752			1089765	57.2752		
	N7097	5.1187	RECLOSER	5.394				
	N7100	5.6692						
	2B4053	56.7519	FUSE654421166	57.1774	2B4053	56.7519	FUSE654421166	57.1774
	2C0234	57.6029			2C0234	57.6029		

From the results we see that even with just two points of measurement the possible candidate nodes for the location of the fault are drastically reduced. Also, the program is able to localize the fault effectively in each case.

Summary:	**Number of cases**	–	**10**
	Success	–	**9**
	Failure	–	**1**

In most cases we see that around 10 nodes are eliminated every time on account of the additional measurement from just one extra location. Also, the fact remains that these eliminated nodes are nodes of high percentage matches and therefore would have been possible candidates had it not been for the additional measurement. Inclusion of additional measurements will further reduce the pool of candidate fault locations thereby identifying the location with an even higher degree of accuracy.

3.4 FLA with Additional Waveforms

If just the addition of additional field monitors that reported just the PD status helped narrow down the fault possibilities so drastically, the next logical step was to include additional waveforms from these measurement points. These waveforms were incorporated as additional inputs into the program.

The model for Feeder 2 proved insufficient for these simulations as it was only able to provide one waveform. A reduced model of the actual feeder was therefore made to overcome this limitation of the previous model. Line impedances from the results of the Thevenin reduction of the system were used to formulate an approximate model considering only those nodes that were of particular interest to the program. These included the point where the fault would be simulated and those locations from where the waveforms needed for the program would be obtained. Refer Figure 3.6 for the model that the actual system was reduced to. The MATLAB

model can be found in the appendix. On comparison with the actual model of the feeder, the reduced model was found to match the results from the actual model to within 10% of the short-circuit analysis values. This error was considered to be an acceptable value and testing was performed on this model.

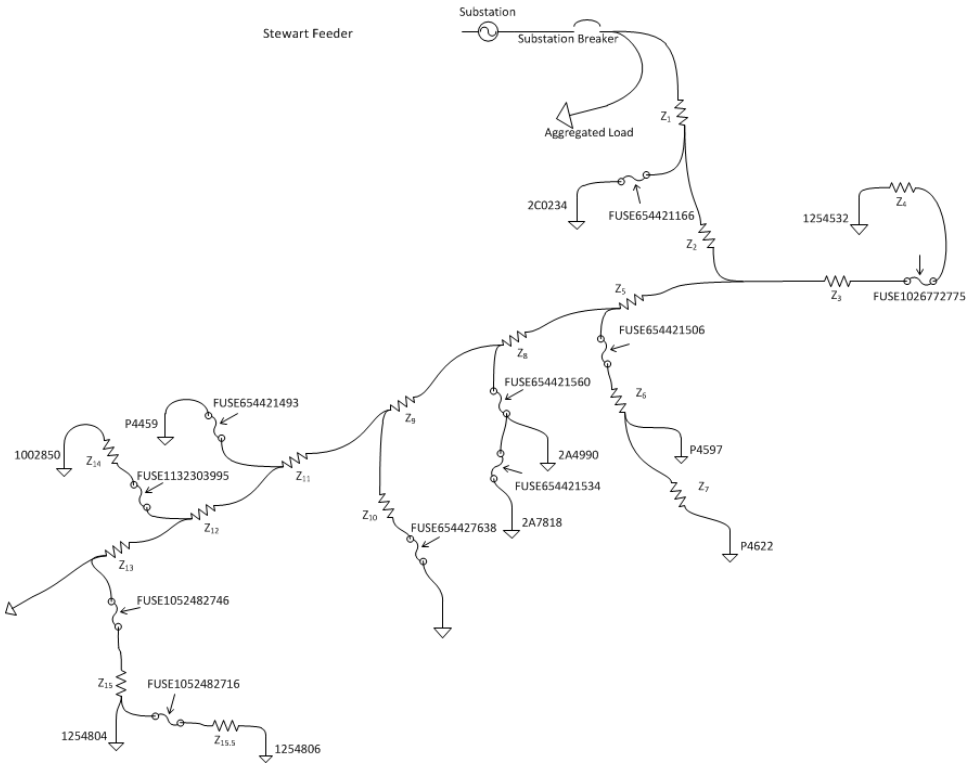

Figure 3.6: Reduced Model

Faults were simulated at each of the nodes on the reduced feeder. These simulations provided the current waveforms from three different places on the feeder for each of the three phases. These waveforms were input to the FLA and the results from the FLA were tabulated. These results have been presented in table 3.6.

Table 3.6: FLA with Additional Waveforms

	Possibilities			
Faulted Node	**Node Name**	**Match**	**Upstream PD**	**PD Match**
2C0234	2C0234	61.01719	FUSE654421166	61.01719
	1130060	56.687499	FUSE654421097	56.687499
	N7088	56.632974	FUSE654421083	56.632974
	1130074	34.125924	FUSE1026772775	34.125924
	N7092	17.150096	RECLOSER	17.153113
	N7093	17.069624		
	1N7525	17.311039		
1254532	1254532	84.766176	FUSE1026772775	84.766176
	P4630	84.510809	FUSE654421480	84.489463
	1T9380	84.446125		
	P4597	82.215521	FUSE654421506	82.215521
	2A7818	81.241753	FUSE654421534	81.241753
	P4646	70.36402	RECLOSER	70.221371
	P4645	70.322623		
	P4634	70.213954		
	1R7856	70.185494		
	P4628	70.118223		
	P4652	70.335559		
	P4679	70.294162		
	P4683	70.250177		
	1248623	70.172557		
	1248625	70.157033		
P4597	P4597	86.791361	FUSE654421506	86.791361

Table 3.6 Continued

	Possibilities			
Faulted Node	**Node Name**	**Match**	**Upstream PD**	**PD Match**
	P4630	85.993591	FUSE654421480	85.993591
	2A7818	85.056416	FUSE654421534	85.056416
	1254532	83.725004	FUSE1026772775	83.725004
	1002422	71.110131	RECLOSER	71.263609
	P4646	71.110131		
	P4645	71.218618		
	P4634	71.33253		
	1R7856	71.362364		
	P4652	71.126404		
	P4679	71.248452		
	P4683	71.29456		
	1248623	71.392198		
P4622	R0712	87.468421	FUSE654421506	87.401736
	P4614	87.465872		
	P4616	87.315512		
	P4622	87.381773		
	P4489	86.25402	FUSE654427653	86.136791
	P4502	86.129145		
	P4508	86.065433		
	P4420	81.306337	FUSE1132303995	81.282551
	P4110	81.283401		
	P4109	81.257916		
	P4392	74.014908	RECLOSER	73.915942
	P4384	73.989423		

Table 3.6 Continued

	Possibilities			
Faulted Node	**Node Name**	**Match**	**Upstream PD**	**PD Match**
	P4391	73.991971		
	P4383	73.956293		
	P4381	73.930808		
	P4380	73.884935		
	P4378	73.86199		
	P4375	73.846708		
	P4238	73.823772		
	P4236	73.805933		
	P4385	40.580445	FUSE654427361	40.541199
	P4387	40.544767		
	P4388	40.514185		
2A4990	2A4990	72.348081	FUSE654421560	72.348081
	P4654	64.847611	FUSE654421375	64.529051
	P4655	64.694877		
	P4660	64.487595		
	P4662	64.36759		
	P4663	64.247585		
	1T9382	63.249782	FUSE654421454	63.249782
	1W6972	61.89522	FUSE654421441	61.772488
	1W6973	61.622481		
	2A7818	47.994279	FUSE654421534	47.994279
1002850	1002850	93.875736	FUSE1132303995	93.875736
	P4268	90.780724	FUSE1052482746	90.780724
	1267645	90.780724		

Table 3.6 Continued

	Possibilities			
Faulted Node	**Node Name**	**Match**	**Upstream PD**	**PD Match**
	P4618	86.783077	FUSE654421506	86.766223
	P4619	86.749369		
	P4513	86.416208	FUSE654427653	86.37501
	P4515	86.404972		
	P4520	86.361152		
	P4522	86.347669		
	P4498	42.225692	FUSE654421586	42.225692
1254806	1254806	77.721721	FUSE1052482716	77.721721
	P4525	71.510215	FUSE654421467	71.510215
	P4524	63.455462	FUSE654427653	63.279203
	P4527	63.276491		
	P4529	63.227681		
	P4530	63.157177		
	1254804	58.469119	FUSE1052482746	58.469119
2A7818	2A7818	67.714362	FUSE654421534	67.714362
	P4630	67.489071	FUSE654421480	67.489071
	P4597	66.947783	FUSE654421506	66.947783
	1254532	65.958347	FUSE1026772775	65.958347
	1002422	60.127744	RECLOSER	60.202021
	P4646	60.127744		
	P4645	60.180247		
	P4634	60.235376		
	1R7856	60.249814		
	P4652	60.135619		

Table 3.6 Continued

	Possibilities			
Faulted Node	**Node Name**	**Match**	**Upstream PD**	**PD Match**
	P4679	60.194686		
	P4683	60.217		
	1248623	60.256377		
	1248625	60.264253		
P4459	P4602	86.837272	FUSE654421506	86.726075
	1E8327	86.794472		
	P4605	86.746636		
	P4607	86.703836		
	P4609	86.648447		
	P4582	85.485107	FUSE654421534	85.485107
	P4459	85.429388	FUSE654421493	85.429388
	P4461	85.452047	FUSE654427653	85.425192
	P4463	85.386587		
	P4536	83.719707	FUSE654427667	83.659283
	P4538	83.641659		
	P4539	83.593824		

Only the top 5 devices with the highest percentage matches are shown.

Summary:	**Number of cases**	–	**9**
	Success	–	**8**
	Failure	–	**1**

Even with the approximate model the program identifies the faulted node and the associated fuse without any trouble. The program gets the location wrong only in one case. Here, as

can be seen the difference in the percentage matches between these locations is a little more than 1 percent. It is believed that a better model will get rid of this discrepancy. Also, with a better model the percentage matches in all the cases will be higher. As was previously stated, the difference between the actual short circuit currents and the ones obtained from the model differ by almost 10 percent. This is the source of the error in the fault location.

As we can see the inclusion of waveforms instead of just the device status helps immensely in reducing the number of likely nodes that the program locates to be the likely locations of the fault on the system. Also, the program identifies the corresponding upstream fuse correctly in each case.

Chapter 4 Sensitivity of FLA to Feeder Model Uncertainties

This chapter presents the additional tests that were performed to determine the sensitivity of FLA to uncertainties that might exist in the model of the distribution feeder. Also, various topologies that were tested to determine the optimal location of the additional monitors on the system are discussed.

To determine the sensitivity, two main tests were performed.

- The impact of fault impedance on the performance of FLA.
- The impact of the variation in load distribution along the feeder on FLA.

4.1 Placement of Additional Field Monitors

Though the provision to include additional measurements may be available, it is infeasible to place PQ monitors at each point on the system. Therefore, these monitors must be strategically placed throughout the system so as to maximize their benefit in locating the faults as they occur.

Multiple strategies were proposed to place these monitors and a couple of them were tested to see their benefits. The various strategies proposed were:

Scheme 1. Placing monitors at locations where the number of downstream nodes is very high without any other protective device in between.

Scheme 2. Placing monitors at locations where FLA with one measurement returned the maximum number of likely faulted locations for a fault at that particular node.

Scheme 3. Placing monitors at those positions that have historically seen a large number of faults when compared to the rest of the system.

Of these strategies, the first and second were tested on Feeder 1 to see how each of these choices influenced the accuracy of the program.

Scheme 1. Measurement from Devices that give Maximum Fault Possibilities

In this case, additional meters were placed at fuses N1 and N14 on the system. These fuses were chosen based on the results obtained from FLA with just one measurement where faults in these devices zones of protection produced the maximum number of likely fault location candidates. These meters gave the status of these fuses back to the program thereby letting the program know if these devices had operated for a particular fault. Once again, faults were simulated throughout the system and the results were tabulated. Fuse N1 and Fuse N14 each have 3 downstream nodes. Table 4.3 presents the results that were obtained when faults were simulated at each of the nodes and FLA was used with additional measurements at fuses N1 and N14 to locate these faults.

Scheme 2. Measurement from Devices that Protect Maximum Downstream Nodes

Next, the second strategy was tested. In this case the position of the meters was at fuses N1 and N142. These are the two fuses that have the maximum number of downstream nodes. Fuse N1 has 3 downstream nodes while Fuse N142 has 5 downstream nodes. Faults were simulated at various nodes and the results were tabulated (Table 4.3).

Table 4.1: Impact of Measurements at Fuses

	Possible Nodes		
Faulted Node	**Basic FLA**	**Measurements at Fuses N1 and N14**	**Measurements at Fuses N1 and N142**
3	3	3	3
	12	12	
4	4	4	4
	12		
5	5	5	5
	6	6	6
	9		
	10		
	17		
6	2	5	5
	5	6	6
	6		
	7		
	10		
	16		
	17		
8	5	8	8
	8	9	17
	9		
	17		
9	5	8	9
	8	9	

Table 4.1 Continued

	Possible Nodes		
Faulted Node	**Basic FLA**	**Measurements at Fuses N1 and N14**	**Measurements at Fuses N1 and N142**
	9		
	17		
10	2	2	10
	6	7	
	7	10	
	10		
	15		
	16		
11	1	1	11
	11	11	
12	3	3	12
	4	12	
	12		
15	2	15	2
	7	16	7
	10		15
	15		16
	16		
16	2	15	2
	6	16	7
	7		15
	10		16
	15		

Table 4.1 Continued

	Possible Nodes		
Faulted Node	**Basic FLA**	**Measurements at Fuses N1 and N14**	**Measurements at Fuses N1 and N142**
	16		
17	5	17	17
	6		
	9		
	10		
	17		

From the tests that have been performed so far it was see that both strategies reduce the number of nodes predicted by the program in their own way. However a distinct conclusion could not be reached as to which strategy is better. Maybe, once additional monitors have been placed on the actual system, it would be possible to perform further tests to determine which strategy of the three would be best suited to maximize the benefit of these additional meters on the system.

4.2 Impact of Fault Impedance on the Systems

To come up with a method for ranking of the results from FLA, a formula was come up with that gives equal importance to the various parameters based on which the conclusions are drawn namely, the fault current magnitude, the load rejection and the time of operation of the protective device.

One of the important factors that impact the fault current levels is the fault impedance.

Table 4.2: Impact of Fault Impedance on the Short Circuit Current

Node	I_F **when** $R_F = 0.001\Omega$ **(A)**	I_F **when** $R_F = 0.3\Omega$ **(A)**
3	1450	1427
4	1365	1350
6	1507	1480
7	1720	1670
13	1440	1425
17	1725	1700

In the fault analysis we usually assume bolted faults. To test how sensitive FLA is to fault resistance, preliminary tests were performed to gauge the impact of the fault impedance on the fault current. It must be noted that these tests do not account for high impedance faults; they are measure of the accuracy of the program to slight deviations from bolted faults. To see what happened the fault impedance was changed from 0.001Ω to 0.3Ω. Using this new value of the fault impedance, short circuit analysis was performed once again to see if it impacted the results drastically. Higher values of fault impedance caused the program difficulties in identifying the fault location.

Table 4.2 shows the fault current magnitudes for both the values of fault impedances. It can be seen that the variations in the magnitude are minimal.

As table 4.2 shows, the change in fault current is not very large when the fault impedance changes. However, to make sure FLA was still able to detect faults accurately the program was run again for faults at these nodes.

Table 4.3: Impact of Measurements at Fuses

Faulted Node	**Nodes Predicted**	**Percentage Match**	**Upstream PD**
3	3	94.2218	N22

Table 4.3 Continued

Faulted Node	Nodes Predicted	Percentage Match	Upstream PD
	12	0.2798	N142
4	3	45.4571	N22
	4	83.5825	N1
	12	74.8189	N142
6	5	85.8395	N1
	6	85.7153	N1
	9	77.5345	N142
	10	78.1162	N142
	17	96.043	N14
7	2	1.5264	N12
	5	1.2053	N1
	6	0.9871	N1
	7	92.9019	N2
	10	0.5666	N142
	17	1.7521	N14
13	13	94.8537	N142
17	5	42.1813	N1
	8	2.4227	N2
	9	32.2864	N142
	17	51.4967	N14

Summary: Number of cases – 6

Success – 5

Failure – 1

As we can see from the results, FLA is still able to determine the location of the fault accurately. This can be attributed to the fact that FLA depends not only on the short circuit current for locating the fault i.e. *Current Error* but also uses the *Time Error* and the *Power Flow Error*. The *Power Flow Error* is independent of the fault impedance and therefore the program is still able to determine the location of the fault accurately.

4.3 Impact of Load Variation

FLA uses power flow analysis to estimate the load that is interrupted by the protective device. This is based on the assumed load distribution on the feeder. Since this distribution may vary from the actual values, it was necessary to figure out the impact that variations in the individual loads at the various nodes have on the FLA. For these tests, the total load on the feeder was kept the same. However, the individual loads were perturbed by a factor of up to 20% from their nominal values. Once again faults were simulated on the system and FLA was run to determine if the program was still able to accurately locate the faults.

Repeated changes in load were made and then the ability of the FLA to accurately determine the location of the fault was verified. The results of these tests were plotted to determine how the program performed each time.

For a fault simulated at Node 2A7818, the FLA returned the following nodes as possible candidate locations for the fault. The nodes highlighted in yellow are those locations that fall under the right fuse that should operate when a fault occurs at Node 2A7818.

1. 'P4642'
2. '1248680'
3. '1248681'
4. '1248681'
5. '1248681'
6. '1254468'
7. '1Y9416'
8. '1Y9416'

9. '1216626'
10. '1216626'
11. '1216626'
12. '1216628'
13. '1216629'
14. '1216630'
15. '1216630'
16. '1Y9416'
17. '2A7744'
18. '2A7744'
19. '1T9382'
20. '1T9382'
21. '1T9382'
22. '1W0136'
23. 'P4628'
24. 'P4624'
25. 'P4592'
26. 'P4591'
27. 'P4585'
28. '2A7818'
29. '2A7818'
30. '2A7819'
31. '2A7820'
32. 'P4585'
33. 'P4580'
34. 'P4594'
35. 'P4597'
36. 'P4597'
37. '1W6973'
38. 'P4663'
39. '1C6533'
40. 'P4665'
41. '1248663'
42. '1248664'
43. '1254860'
44. '2050951'
45. '2050951'
46. '2050952'
47. '1130074'
48. '1254532'
49. '1254532'
50. '1254532'
51. '1254533'
52. '1254531'
53. '1254531'
54. '2051112'
55. '1254531'
56. '2050966'
57. '1254530'
58. '1254528'
59. '2050943'
60. '2050943'
61. '2050952'
62. '2050963'
63. '1254539'
64. '1267897'
65. '1267897

Figure 4.1 shows the percentage matches for the list of nodes above when the load is varied around the nominal by a factor of 10 percent. As can be seen, in this case, the program has no trouble locating the right fuse and the right node in each case.

Similarly, figure 4.2 shows the percentage matches for a 20 percent variation in load off the nominal load on the feeder. In this case, we see that sometimes FLA shows other nodes with

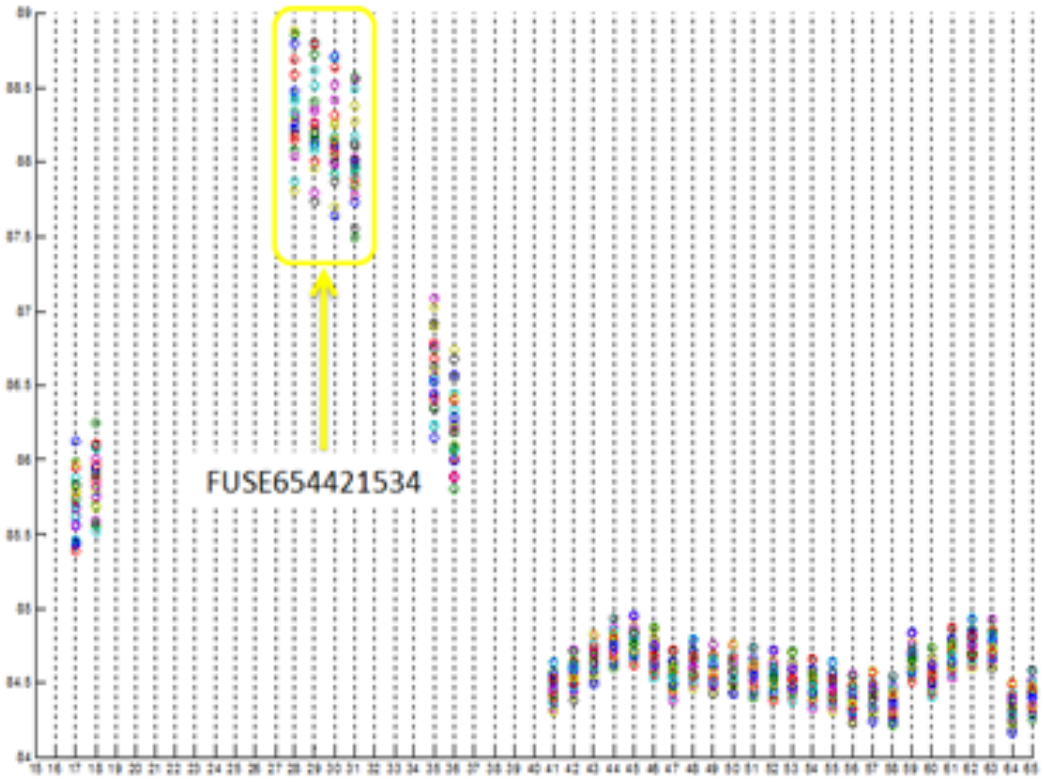

Figure 4.1: Results for 10% Load Variation (Showing Nodes with over a 80% Match)

percentage matches comparable to those at the point of the fault.

These tests were repeated for the various nodes in the system. For each case, the load was varied by both 10 and 20 percent off the nominal value and the output from FLA for each set of power flow values was calculated. These values were plotted as graphs each accompanied by its list of nodes.

These figures for the other cases can be found in the appendix. Preliminary tests showed that for some cases the impact of these changes in load were minimal. The program was able to identify the faulted node without any problems. For the others, there was some confusion as to which node was most likely to be faulted.

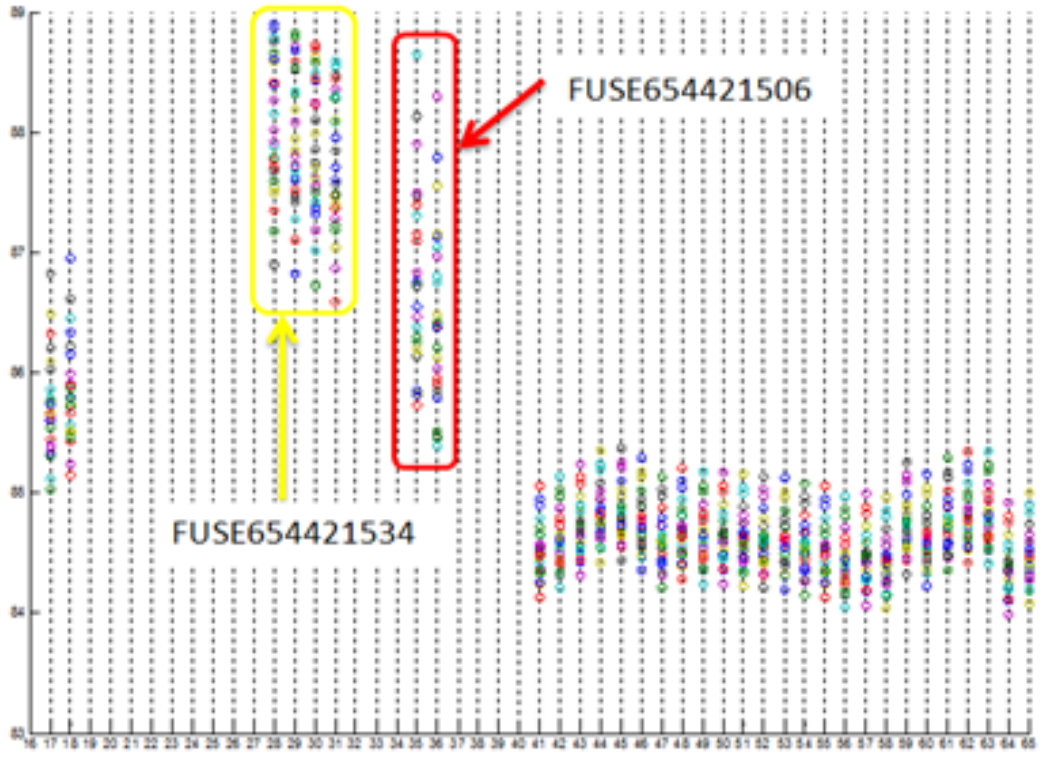

Figure 4.2: Results for 20% Load Variation (Showing Nodes with over a 80% Match)

To determine the likelihood of the program identifying the node correctly, those cases where the program showed many nodes with close percentage matches to the faulted node were tested again. But this time a success table was created to see how many times the program identified the faulted node correctly. Also, if the program was unable to successfully identify the faulted node, the results were studied to see what could be done to rectify these issues. A total of 28 trials were performed for each of these nodes and the results were tabulated. Refer table 4.4 to see the results of both Baisc FLA and FLA with additional measurements.

Table 4.4: Impact of Load Variation on the FLA

Faulted Node	10% Load Variation				20% Load Variation			
	Additional Measurements		Basic FLA		Additional Measurements		Basic FLA	
	Success	**Failure**	**Success**	**Failure**	**Success**	**Failure**	**Success**	**Failure**
2C0234	12	16	11	17	12	16	16	12
2A7818	28	0	28	0	24	4	23	5
P4241	28	0	28	0	28	0	28	0
P4459	11	17	9	19	18	10	17	11
P4597	27	1	27	1	14	14	19	9
P4622	28	0	28	0	26	2	24	4

Table 4.5: Impact of Load Variation - Node 2C0234

Faulted Node	10% Load Variation		20% Load Variation	
	Success	**Failure**	**Success**	**Failure**
2C0234	29	32	41	20

Using the data from these results, the following conclusions were drawn based on the simulations and the individual nodes. Through the testing that has performed done so far it was found that the correct fuse was always within the top 4 fuses identified by the program. Also, when the program gets the fuse wrong, the fuse that the program determines is always within close geographical proximity of the right fuse.

1. 2C0234:

   10% Load Variation The maximum difference of percentage matches was around 2% between the right fuse and the one the program predicted.

   20% Load Variation The maximum difference of percentage matches was around 3% between the right fuse and the one the program predicted.

   Since the 20% load variation showed a better performance than the 10% load variation additional cases were tested to see why this was the case. An additional 61 cases were tested.

   In both cases the program localizes the fault accurately. The nodes predicted by the program are right next to each other on the feeder. The reason why the program gets the identification wrong in some cases is due to the fact that the nodes that are predicted a fuse of the same rating protecting them (40T fuses in this case.) Also the current flow through the two fuses is almost the same (12.11A in one and 12.13A in the other.) The almost similar current flow also causes the program to perform better when the load variation is

higher as can be seen from the results for the 20 percent load variation when compared with the 10 percent load variation in table 4.5. The variation increases the difference between the current flows in these two fuses and therefore the program performs better with the higher load variation in this case.

2. 2A7818:

   10% Load Variation The program identified the right fuse correctly every time.

   20% Load Variation The maximum difference of percentage matches was less than 1% between the right fuse and the one the program predicted.

3. P4241:

   10% Load Variation The program identified the fuse correctly.

   20% Load Variation The program identified the fuse correctly.

4. P4459:

   10% Load Variation The maximum difference of percentage matches was around 2% between the right fuse and the one the program predicted.

   20% Load Variation The maximum difference of percentage matches was around 2% between the right fuse and the one the program predicted.

   Since 20% load variation showed better performance than 10% load variation additional cases were tested to verify the performance of the program. An additional 61 cases were tested and the results have been tabulated (table 4.6.)

   The program gets the node wrong in some cases and predicts the incorrect node since both sets of predicted nodes are protected by the same kind of fuse (65T fuses in this case) and also their short circuit currents are the same (around 1675A for both sets of nodes.) Therefore the program has only the *Power Flow Error* to determine the ranking for the nodes.

Table 4.6: Impact of Load Variation - Node P4459

Faulted Node	10% Load Variation		20% Load Variation	
	Success	Failure	Success	Failure
P4459	35	26	29	32

5. P4597:

   10% Load Variation The maximum difference of percentage matches was less than 1% between the right fuse and the one the program predicted for the one case where the program identified the fuse incorrectly.

   20% Load Variation The maximum difference of percentage matches was around 2% between the right fuse and the one the program predicted.

6. P4622:

   10% Load Variation The program identified the fuse correctly.

   20% Load Variation The maximum difference in percentage matches was around 1.5% between the right fuse and the one the program predicted.

Based on the results obtained from these tests, it is recommended that power flow analysis be run each time a fault event occurs based on the data available about the pre-fault condition of the system. This way, most discrepancies can be avoided. If however such data is not accurately available, of the locations determined by the program one of the top four fuses is always the location of the fault. Thus, even if the program does not explicitly determine the fault location accurately, it is still able to localize the fault pretty well.

Chapter 5 Conclusions

In conclusion, this chapter gives a summary of the tests that were performed on FLA using the various feeder models and the results that were obtained up on the performance of these tests.

The chapter outlines the work that could be performed to improve the performance of the program in the future.

5.1 Summary

FLA was comprehensively tested and the results have been presented. The program is able to identify the fault location accurately whenever the waveform from a permanent fault is provided.

Tests were performed on the smaller feeder and also on a model of the feeder provided by Allegheny Power Inc. Basic FLA that made use of just one current waveform as well as FLA with multiple field monitors that provided just the PD status and current waveforms from these locations were tested and the results were presented.

On Feeder 1 Case 1, Basic FLA had a success rate of 8 out of 12 correct identification for faults simulated. For Case 2, the presence of fuses improved the success rate of faulted node identification to 11 out of 12 for faults simulated. When FLA with additional monitors was tested in both cases the success rate was 12 out of 12 for fault location identification.

On Feeder 2, both Basic FLA and FLA with additional monitors succeeded in identifying the faulted node 9 out of 10 times. However, Basic FLA gives a long list of possibly faulted nodes to sift through before arriving at the right node. When additional monitors are used this list is greatly reduced and fault location becomes easier.

FLA with additional waveforms was tested on Feeder 2 and it was found that the program identified the faulted node correctly 8 out of 9 times. In the one instance where the program identified the faulted node incorrectly, both nodes were close to each other geographically.

Two techniques on where to place the additional field monitors were tested. Based on these tests it could not be decided which is the best scheme to use on the feeder to derive the maximum benefit from the additional monitors that provide data for the program in addition to the monitors at the substation. The impact of changes in fault impedances on the fault current and thereby on the performance of the program was studied and their implications presented.

Also, the effect load variations would have on the accuracy of the program has been studied. These results were also presented in detail.

5.2 Future Work

Once these additional monitors are placed on the field, a more thorough testing of the system can be done. Also, if possible the position of these devices can be changed based on the performance of the program to a particular set of locations, this increasing the benefits obtained from these additional measurements. Scheme 3 for the placement of additional measurements on the feeder can be tested once the basic system returns data and the most fault-prone locations are determined. Thereby, based on the results obtained, the optimal locations of these meters on the system can be determined.

Another scheme for the placement could be where monitors are placed in locations where laterals are protected by the same kind of fuse and also have similar power flows under normal operating conditions. Therefore, the program could use the additional data to improve its localization of the faulted node.
Using the results from the field, adjustments to the ranking could be made as required to further

improve the accuracy of the program in locating the faults. Also, instead of using the absolute error to determine the rankings, the method of least squares could be used which would allow for ranking the nodes based on different weighting factors for the different calculated errors.

Presently, the program determines the fault locations and then eliminates the improbable ones based on the additional measurements obtained from the meters. This means that the program determines the list of faulted nodes from all the nodes in the system. To speed up the fault location process, a future version of FLA could eliminate nodes first by checking if the currents through the additional meters are over the threshold levels for a fault. In this way, parts of the feeder downstream of these meters can be removed from consideration so that the program has less data to sort through, thereby speeding up the program.

An interesting addition that could be made once data from a substantial number of cases becomes available is the calculation of compensation factors to account for any discrepancies that might exist in the model of the system in the software when compared to the actual feeder.

REFERENCES

[1] T. Dillon and M. Laughton. Expert System Application in Power Systems. 1990.

[2] H. Hooshyar. *System Protection for High PV-Penetrated Residential Distribution Systems (Green Hubs).* PhD thesis, North carolina State University, Raleigh, 2011.

[3] P. Crossley J. Tan and Kirschen D. Fault Section Identification on a Transmission Network Using Factors and Expert System Technology. *Proceedings of 13th Power Systems Computations Conference - PSCC, Trondheim*, 1999.

[4] C. Kim and B. Russel. Classification of Faults and Switching Events by Inductive Reasoning and Expert System Technology. *IEEE Transactions on Power Delivery*, 4:1631–1637, 1989.

[5] Jinsang Kim, M.E. Baran, and G.C. Lampley. Estimation of fault location on distribution feeders using pq monitoring data. *IEEE Power Engineering Society General Meeting, 2007.*

[6] F. Provoost M. M. Saha and E. Rosolowski. Fault Location Method for MV Cable Network. *DPSP, Amsterdam, The Netherlands*, April, 2001.

[7] J. Izykowski M. M. Saha and E. Rosolowski. *Fault Location on Power Networks.* Springer-Verlag London Limited, 2010.

[8] P. Verho M. M. Saha, R. Das and D. Novosel. Review of Fault Location Techniques for Distribution Systems. *Power Systems and Communications Infrastructures for the Future, Beijing*, 2002.

[9] N. Karnik S. Das, S. Kulkarni and S. Santoso. Distribution fault location using short-circuit fault current profile approach. *Power Engineering Society, IEEE General Meeting - PES*, 2011.

[10] J. Smith. Progress Reports - Fault Location on Distribution Feeders. *Raleigh, North Carolina*, 2011.

APPENDICES

Chapter A Figures of the Systems used in Testing

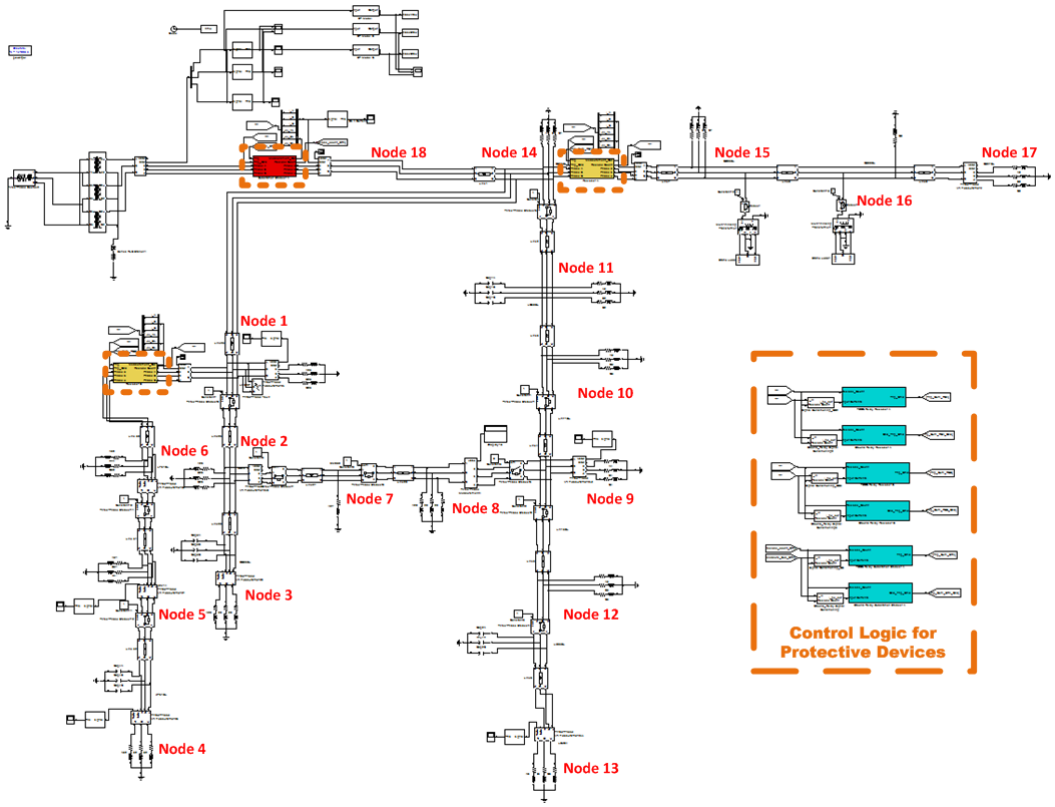

Figure A.1: Feeder 1 - Case 1 - 1 Circuit Breaker (Red) and 2 Reclosers (Yellow)

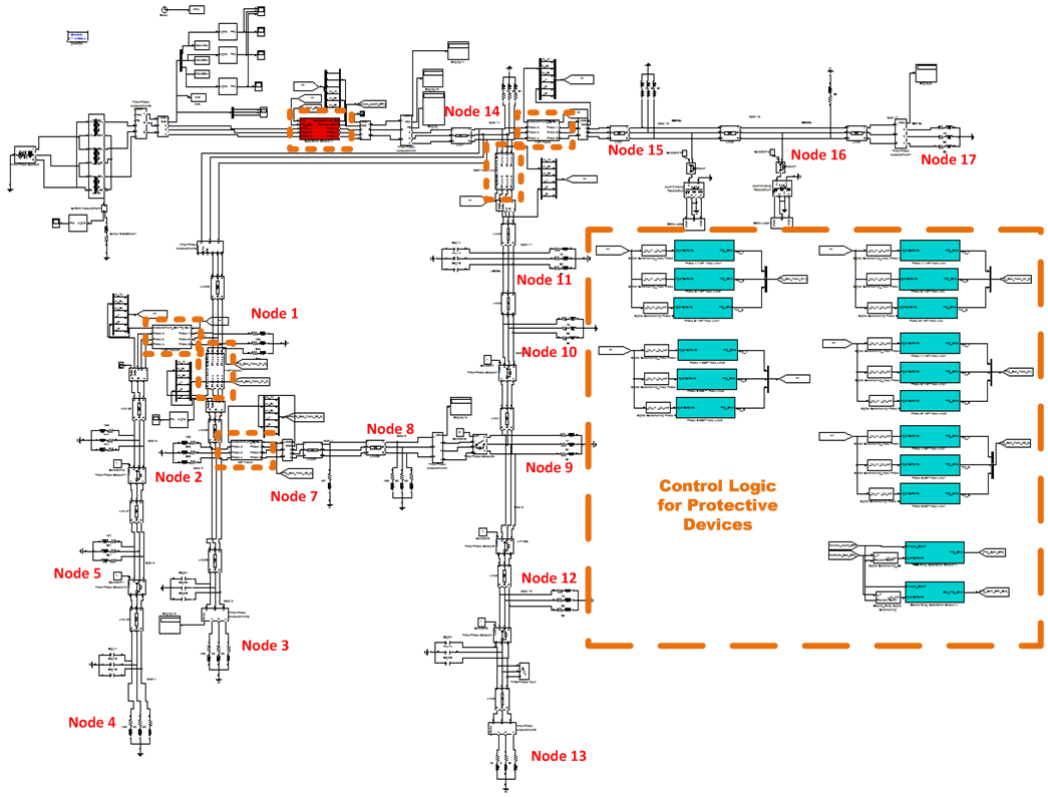

Figure A.2: Feeder 1 - Case 1 - 1 Circuit Breaker (Red) and 5 Fuses (White)

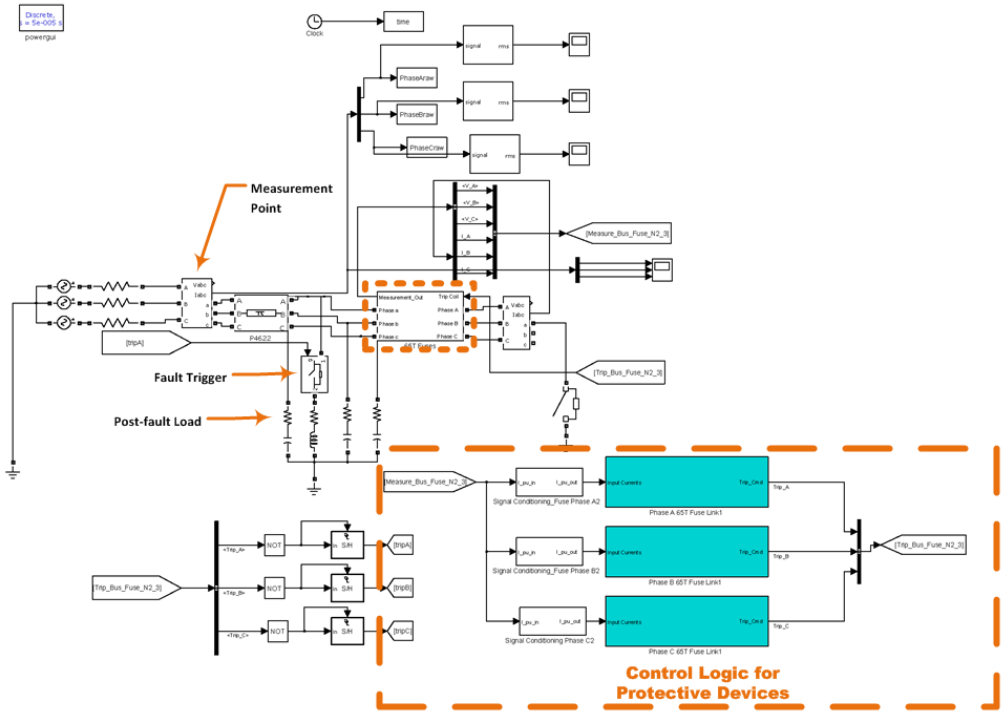

Figure A.3: Feeder 2 - Equivalent Circuit for a Faulted Region

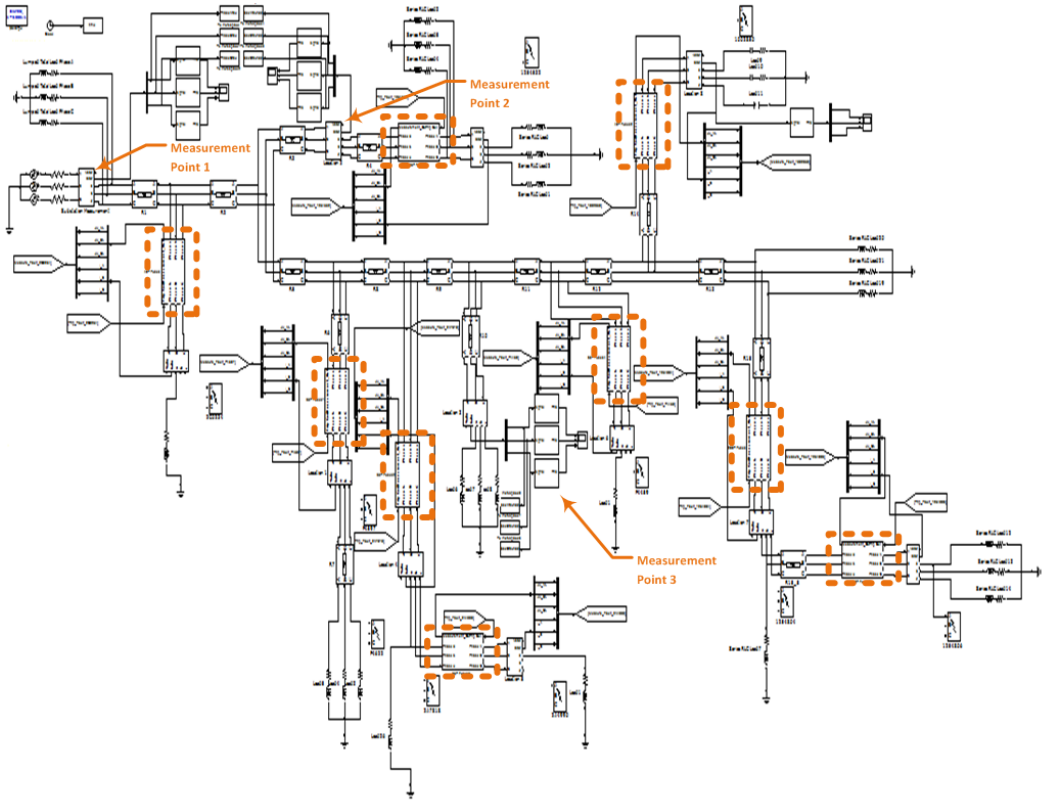

Figure A.4: Reduced System 9 Fuses and 3 Measurement Points

Chapter B Sample Fault Locator Output

```
-----------------------------------------------------
The most likely device(s) to have isolated the fault:


-----------------------------
Device: FUSE1026772775
Percentage Match: 88.605043%
-----------------------------
Fault Point 1248663:
Likelihood of Fault Being @ this Point: 86.232667%
Fault Point 1248663:
Likelihood of Fault Being @ this Point: 86.232667%
Fault Point 1248663:
Likelihood of Fault Being @ this Point: 86.215793%
Fault Point 1254532:
Likelihood of Fault Being @ this Point: 93.361016%
Fault Point 1254532:
Likelihood of Fault Being @ this Point: 93.361016%
Fault Point 1254532:
Likelihood of Fault Being @ this Point: 93.361016%
Fault Point 1267897:
Likelihood of Fault Being @ this Point: 86.228685%
Fault Point 1267897:
Likelihood of Fault Being @ this Point: 86.220654%
Fault Point 1267880:
Likelihood of Fault Being @ this Point: 86.231872%

-----------------------------
Device: FUSE654421560
Percentage Match: 53.101642%
-----------------------------
Fault Point 2A4990:
Likelihood of Fault Being @ this Point: 53.101642%
Fault Point 2A4990:
Likelihood of Fault Being @ this Point: 53.101642%

-----------------------------
Device: FUSE654421375
Percentage Match: 52.016218%
-----------------------------
Fault Point P4654:
Likelihood of Fault Being @ this Point: 52.059760%
Fault Point P4655:
Likelihood of Fault Being @ this Point: 52.039524%
Fault Point P4660:
Likelihood of Fault Being @ this Point: 52.011081%
Fault Point P4662:
Likelihood of Fault Being @ this Point: 51.994073%
Fault Point P4663:
Likelihood of Fault Being @ this Point: 51.976651%

-----------------------------
Device: FUSE654421454
```

```
Percentage Match: 51.838308%
------------------------------
Fault Point 1T9382:
Likelihood of Fault Being @ this Point: 51.838308%
Fault Point 1T9382:
Likelihood of Fault Being @ this Point: 51.838308%

------------------------------
Device: FUSE654421441
Percentage Match: 51.634185%
------------------------------
Fault Point 1W6972:
Likelihood of Fault Being @ this Point: 51.651404%
Fault Point 1W6972:
Likelihood of Fault Being @ this Point: 51.649157%
Fault Point 1W6972:
Likelihood of Fault Being @ this Point: 51.623183%
Fault Point 1W6973:
Likelihood of Fault Being @ this Point: 51.612996%

------------------------------
Device: FUSE654421534
Percentage Match: 49.722216%
------------------------------
Fault Point 2A7818:
Likelihood of Fault Being @ this Point: 49.722216%
Fault Point 2A7818:
Likelihood of Fault Being @ this Point: 49.722216%

------------------------------
Device: FUSE654421506
Percentage Match: 49.546660%
------------------------------
Fault Point P4597:
Likelihood of Fault Being @ this Point: 49.546660%
Fault Point P4597:
Likelihood of Fault Being @ this Point: 49.546660%

------------------------------
Device: FUSE654421480
Percentage Match: 49.458693%
------------------------------
Fault Point P4630:
Likelihood of Fault Being @ this Point: 49.465032%
Fault Point P4630:
Likelihood of Fault Being @ this Point: 49.465032%
Fault Point P4630:
Likelihood of Fault Being @ this Point: 49.458928%
Fault Point 1T9380:
Likelihood of Fault Being @ this Point: 49.445779%

------------------------------
Device: RECLOSER
```

```
Percentage Match: 47.572288%
-----------------------------
Fault Point P4645:
Likelihood of Fault Being @ this Point: 47.609717%
Fault Point P4634:
Likelihood of Fault Being @ this Point: 47.579104%
Fault Point 1R7856:
Likelihood of Fault Being @ this Point: 47.570858%
Fault Point P4628:
Likelihood of Fault Being @ this Point: 47.550975%
Fault Point P4628:
Likelihood of Fault Being @ this Point: 47.532910%
Fault Point 1R7856:
Likelihood of Fault Being @ this Point: 47.576864%
Fault Point P4679:
Likelihood of Fault Being @ this Point: 47.601830%
Fault Point P4683:
Likelihood of Fault Being @ this Point: 47.589460%
Fault Point P4683:
Likelihood of Fault Being @ this Point: 47.589460%
Fault Point P4683:
Likelihood of Fault Being @ this Point: 47.570103%
Fault Point 1248623:
Likelihood of Fault Being @ this Point: 47.567077%
Fault Point 1248625:
Likelihood of Fault Being @ this Point: 47.562514%
Fault Point 1248625:
Likelihood of Fault Being @ this Point: 47.548644%
Fault Point 1248625:
Likelihood of Fault Being @ this Point: 47.562514%

-----------------------------
Device: FUSE1033797688
Percentage Match: 44.834297%
-----------------------------
Fault Point 1248662:
Likelihood of Fault Being @ this Point: 44.836247%
Fault Point 1248662:
Likelihood of Fault Being @ this Point: 44.832346%

-----------------------------
Device: FUSE1030994040
Percentage Match: 44.813047%
-----------------------------
Fault Point 1248681:
Likelihood of Fault Being @ this Point: 44.813842%
Fault Point 1248681:
Likelihood of Fault Being @ this Point: 44.812251%

-----------------------------
Device: FUSE1147838285
Percentage Match: 44.774908%
-----------------------------
```

```
Fault Point P4641:
Likelihood of Fault Being @ this Point: 44.790961%
Fault Point P4641:
Likelihood of Fault Being @ this Point: 44.758855%

------------------------------
Device: FUSE654421402
Percentage Match: 44.741610%
------------------------------
Fault Point P4641:
Likelihood of Fault Being @ this Point: 44.790961%
Fault Point P4641:
Likelihood of Fault Being @ this Point: 44.758855%
Fault Point P4642:
Likelihood of Fault Being @ this Point: 44.736856%
Fault Point P4642:
Likelihood of Fault Being @ this Point: 44.720489%
Fault Point 1248680:
Likelihood of Fault Being @ this Point: 44.714949%
Fault Point P4642:
Likelihood of Fault Being @ this Point: 44.727550%

------------------------------
Device: FUSE654421415
Percentage Match: 44.417054%
------------------------------
Fault Point P4636:
Likelihood of Fault Being @ this Point: 44.422199%
Fault Point P4636:
Likelihood of Fault Being @ this Point: 44.411909%
>>
```

Chapter C Comprehensive Details of Load Variation

It was decided to determine the impact of load variation on the performance of the program. To go about this, the load flow through the protective devices was changed by up to 20 percent while keeping the total load on the system the same. Multiple trials were run, the results of which have been presented below.

C.1 Fault at 2C0234 - Possibly Faulted Nodes

1. '1063612'
2. '1130060'
3. '1076088'
4. 'no local name'
5. 'N7094'
6. '1077826'
7. '1089765'
8. 'N7095'
9. 'N7095'
10. 'N7097'
11. '2B4053'
12. '2B4053'
13. '2C0234'
14. '2C0234'
15. 'N7097'
16. 'N7100'
17. 'N7100'
18. 'N7101'
19. 'N7101'
20. '1130074'
21. '1130074'
22. 'no local name'
23. 'N7072'
24. 'N7072'
25. '1J2763'
26. '1J2763'
27. 'N7072'
28. 'N7071'
29. 'N7070'
30. '3A2054'
31. '3A2054'
32. 'N7068'

C.2 Fault at 1254806 - Possibly Faulted Nodes

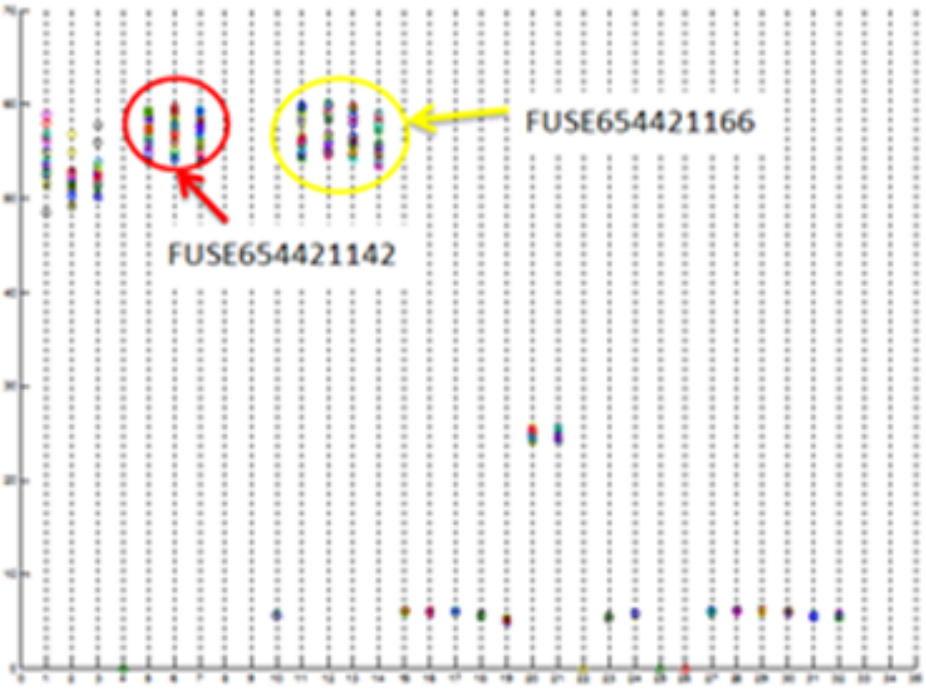

Figure C.1: 2C0234 - Results for 10% Load Variation

1. P4495'
2. 'P4496'
3. 'P4496'
4. 'P4498'
5. 'P4498'
6. 'P4502'
7. 'P4508'
8. 'P4509'
9. 'P4509'
10. 'P4513'
11. 'P4513'
12. 'P4388'
13. 'P4378'
14. 'P4375'
15. 'P4238'
16. 'P4236'
17. 'P4236'
18. 'P4235'
19. 'P4235'
20. '1279017'
21. '1279017'
22. '1279017'
23. '1279017'
24. 'N7970'
25. 'N7970'
26. 'N7955'
27. 'N7955'
28. 'N7955'
29. '1063586'
30. 'N7972'
31. 'N7972'
32. 'N7973'
33. 'N7974'
34. 'N7974'
35. '1L5936'
36. 'N7976'

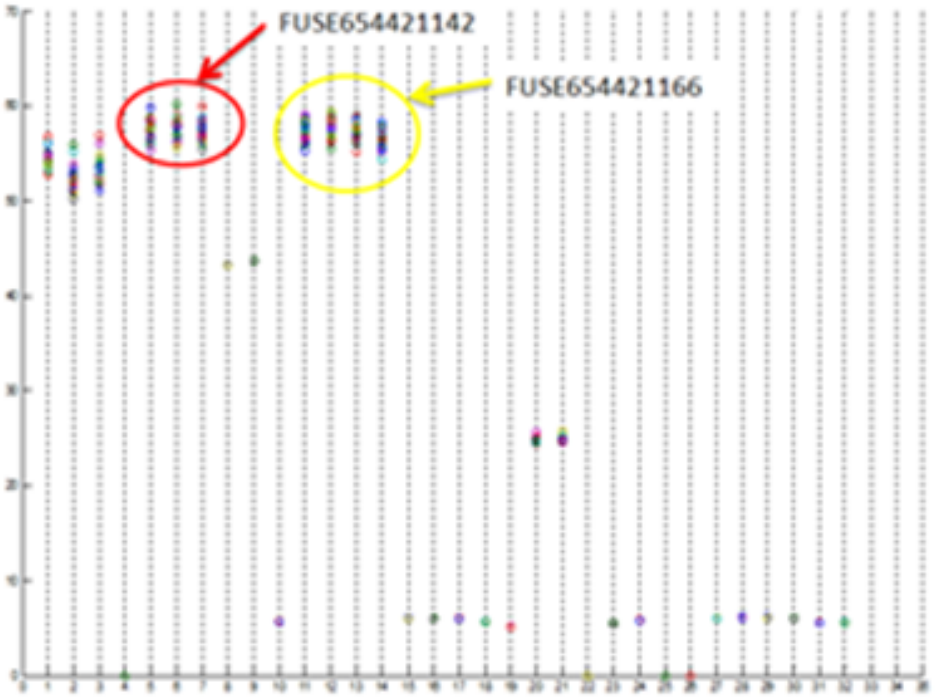

Figure C.2: 2C0234 - Results for 20% Load Variation

37. 'P4240'
38. 'P4241'
39. 'P4241'
40. 'P4247'
41. 'P4247'
42. '1254805'
43. '1254804'
44. '1254804'
45. 'P4266'
46. '1254806'
47. '1254806'
48. '1254807'
49. '1254808'
50. '1254809'
51. 'P4268'
52. '1267645'
53. 'P4560'
54. '1254568'
55. 'P4616'
56. 'P4616'
57. 'P4618'

C.3 Fault at P4241 - Possibly Faulted Nodes

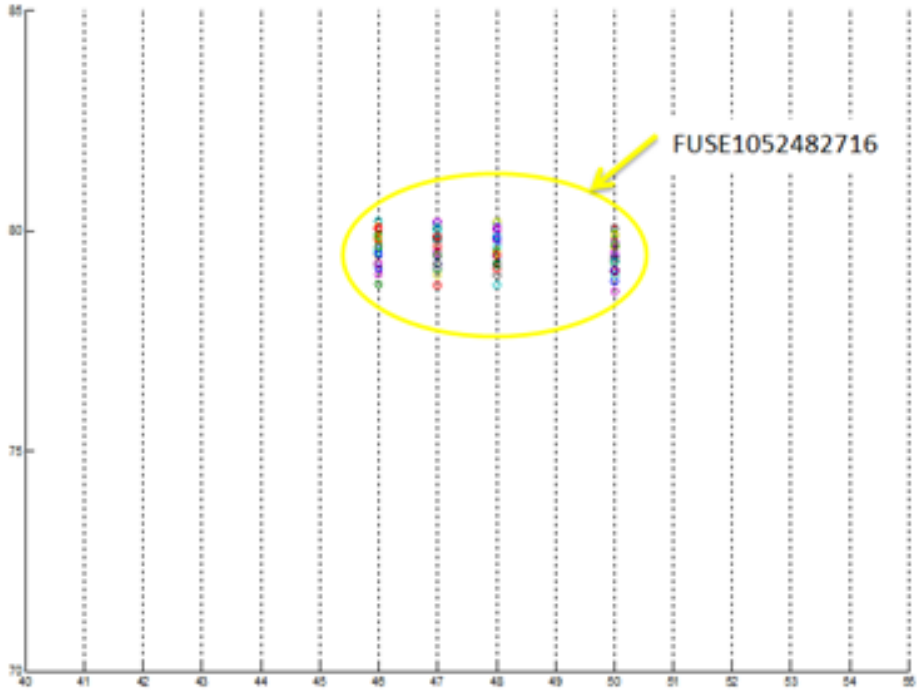

Figure C.3: 1254806 - Results for 10% Load Variation (Showing Nodes with over a 70% Match)

1. 'P4496'
2. 'P4496'
3. 'P4498'
4. 'P4498'
5. 'P4509'
6. 'P4509'
7. 'P4513'
8. 'P4513'
9. 'P4515'
10. 'P4515'
11. 'P4236'
12. 'P4236'
13. 'P4235'
14. 'P4235'
15. '1279017'
16. '1279017'
17. '1279017'
18. '1279017'
19. 'N7970'
20. 'N7970'
21. 'N7955'
22. 'N7955'
23. 'N7955'
24. '1063586'
25. 'N7972'
26. 'N7972'
27. 'N7973'
28. 'N7974'
29. 'N7974'
30. '1L5936'
31. 'N7976'
32. 'N7976'
33. 'N7977'
34. 'N7977'
35. 'P4240'
36. 'P4241'

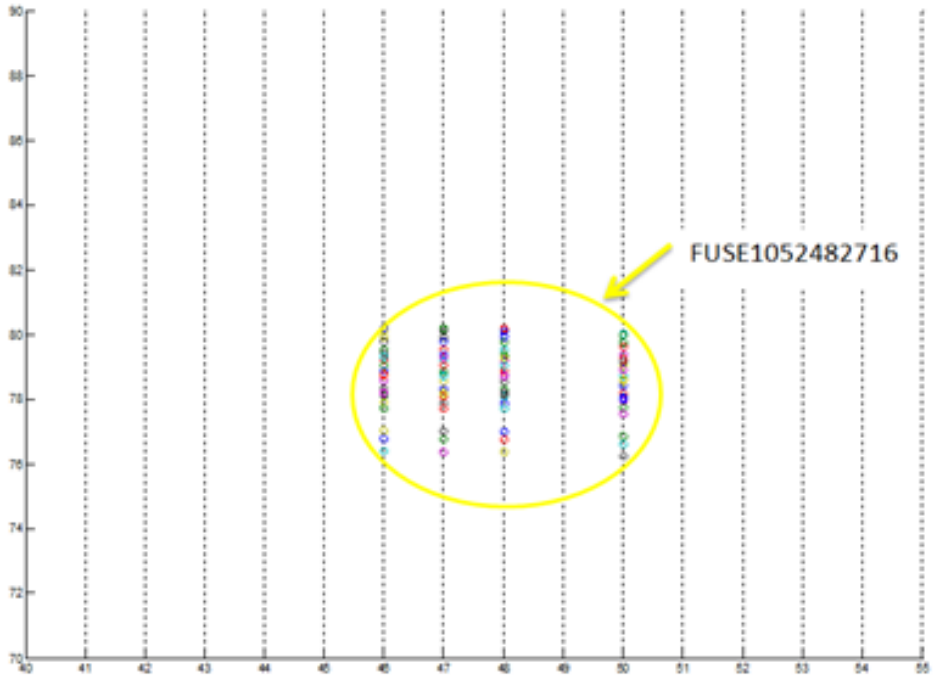

Figure C.4: 1254806 - Results for 20% Load Variation (Showing Nodes with over a 70% Match)

37. 'P4241'
38. 'P4247'
39. 'P4247'
40. '1254805'
41. '1254804'
42. '1254804'
43. 'P4266'
44. '1254806'
45. '1254806'
46. '1254807'
47. '1254808'
48. '1254809'
49. 'P4268'
50. '1267645'
51. 'P4616'
52. 'P4618'
53. 'P4619'

C.4 Fault at P4459 - Possibly Faulted Nodes

1. '1216630'
2. '2A7820'
3. '1248612'
4. 'P4582'
5. 'P4582'
6. 'P4582'
7. '2A4990'
8. '2A4990'

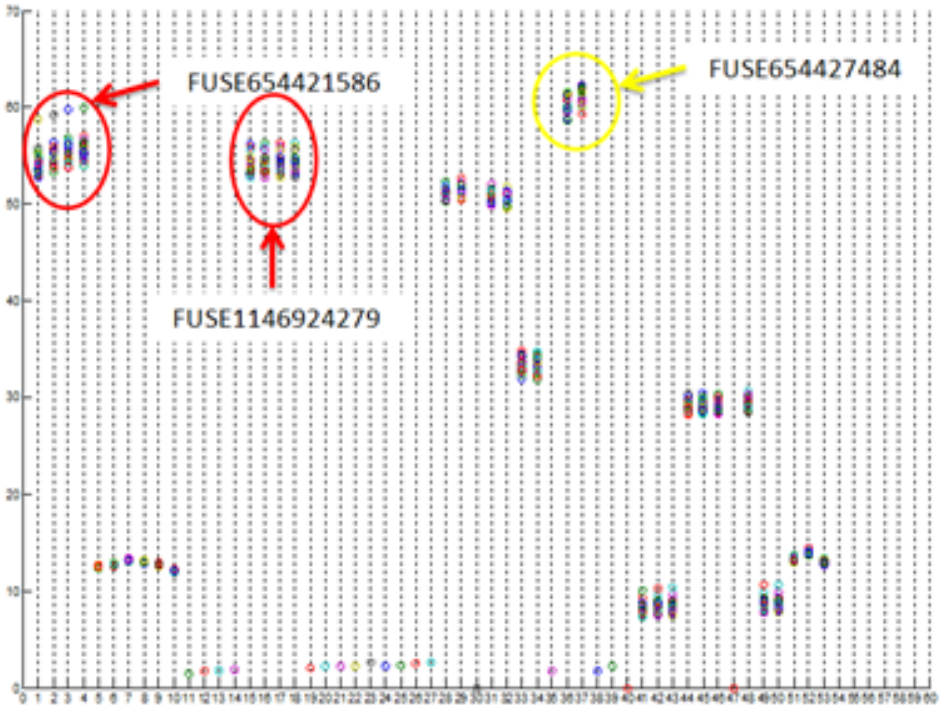

Figure C.5: P4241 - Results for 10% Load Variation

9. 'P4580'
10. 'P4579'
11. 'P4579'
12. 'P4579'
13. 'P4577'
14. 'P4574'
15. 'P4574'
16. 'P4535'
17. 'P4535'
18. 'P4536'
19. 'P4536'
20. 'P4459'
21. 'P4459'
22. 'P4459'
23. 'P4461'
24. 'P4461'
25. 'P4463'
26. 'P4458'
27. 'P4457'
28. 'P4457'
29. 'P4453'
30. '2A7715'
31. '2A7715'
32. 'P4451'
33. 'P4451'
34. 'P4406'
35. 'P4406'
36. 'P4406'
37. 'P4408'
38. 'P4405'
39. 'P4543'
40. 'P4543'
41. 'P4543'
42. 'P4544'
43. 'P4544'
44. 'P4545'

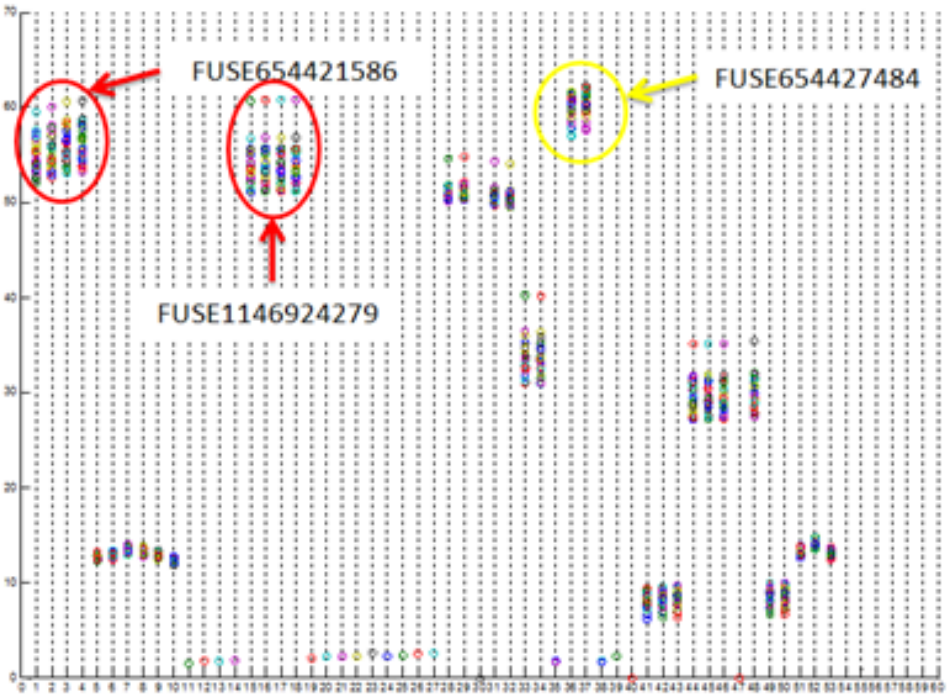

Figure C.6: P4241 - Results for 20% Load Variation

45. 'P4597'
46. '1002869'
47. 'P4602'
48. '1E8327'
49. 'P4605'
50. 'P4607'
51. '2050966'
52. '1254530'
53. '1254528'
54. '1254859'

C.5 Fault at P4597 - Possibly Faulted Nodes

1. 'P4642'
2. '1248680'
3. '1248681'
4. '1248681'
5. '1248681'
6. '1254468'
7. 'P4642'
8. '1T9380'
9. '1Y9416'
10. '1Y9416'
11. '1216626'
12. '1216626'
13. '1216626'
14. '1216628'
15. '1216629'
16. '1216630'

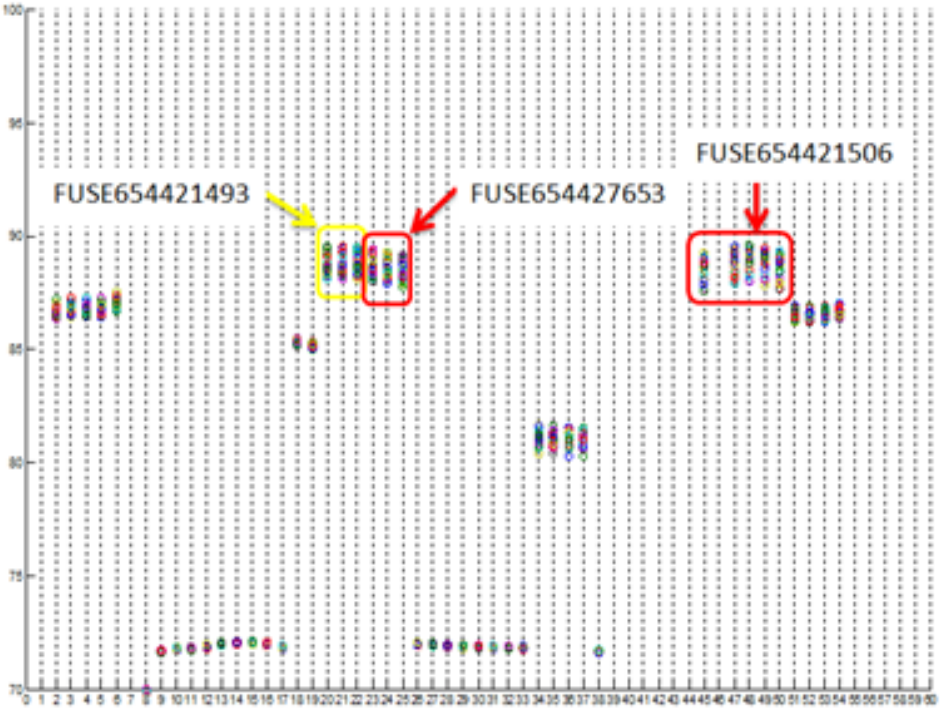

Figure C.7: P4459 - Results for 10% Load Variation (Showing Nodes with over a 70% Match)

17. '1216630'
18. '1Y9416'
19. '2A7744'
20. '2A7744'
21. '1T9382'
22. '1T9382'
23. '1T9382'
24. '1W0136'
25. 'P4628'
26. 'P4624'
27. 'P4592'
28. 'P4591'
29. 'P4585'
30. '2A7818'
31. '2A7818'
32. '2A7819'
33. 'P4585'
34. 'P4594'
35. 'P4597'
36. 'P4597'
37. '1W6972'
38. '1W6973'
39. 'P4662'
40. 'P4663'
41. '1C6533'
42. 'P4665'
43. '1248625'
44. '1248663'
45. '1248663'
46. '1248663'
47. '1248664'
48. '1254860'
49. '2050951'
50. '2050951'
51. '2050952'
52. '1130074'

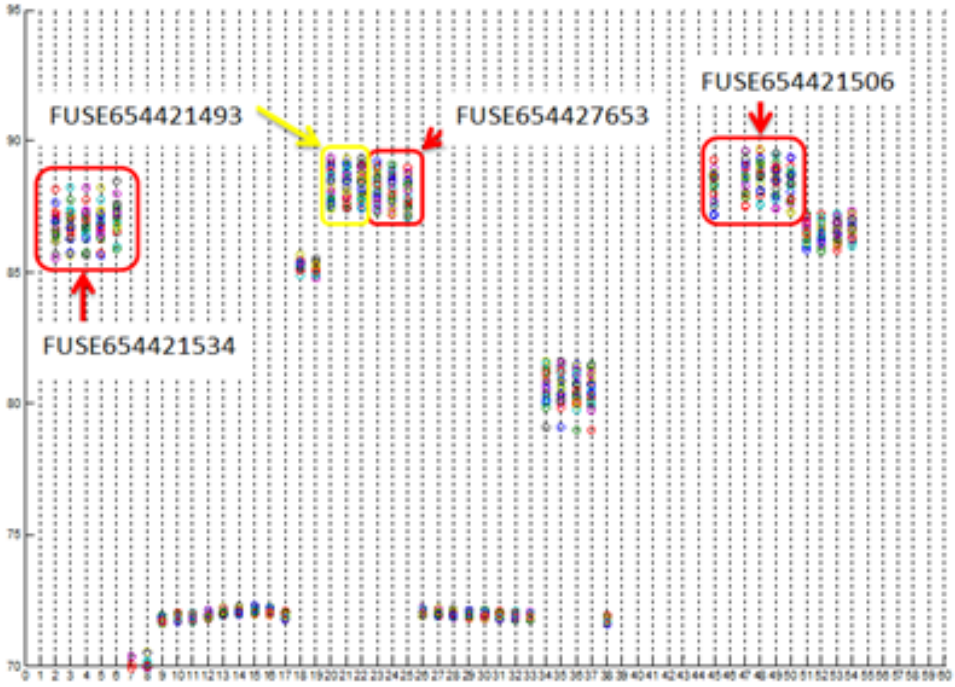

Figure C.8: P4459 - Results for 20% Load Variation (Showing Nodes with over a 70% Match)

53. '1254532'
54. '1254532'
55. '1254532'
56. '1254533'
57. '1254531'
58. '1254531'
59. '2051112'
60. '1254531'
61. '2050943'
62. '2050943'
63. '2050952'
64. '2050963'
65. '1254539'
66. '1267897'
67. '1267897'
68. '1267880'
69. '1248662'
70. '1248662'

C.6 Fault at 2A4990 - Possibly Faulted Nodes

1. '1248681'
2. '1254468'
3. '1216626'
4. '1216626'
5. '1216628'
6. '1216629'
7. '1216630'
8. '1216630'

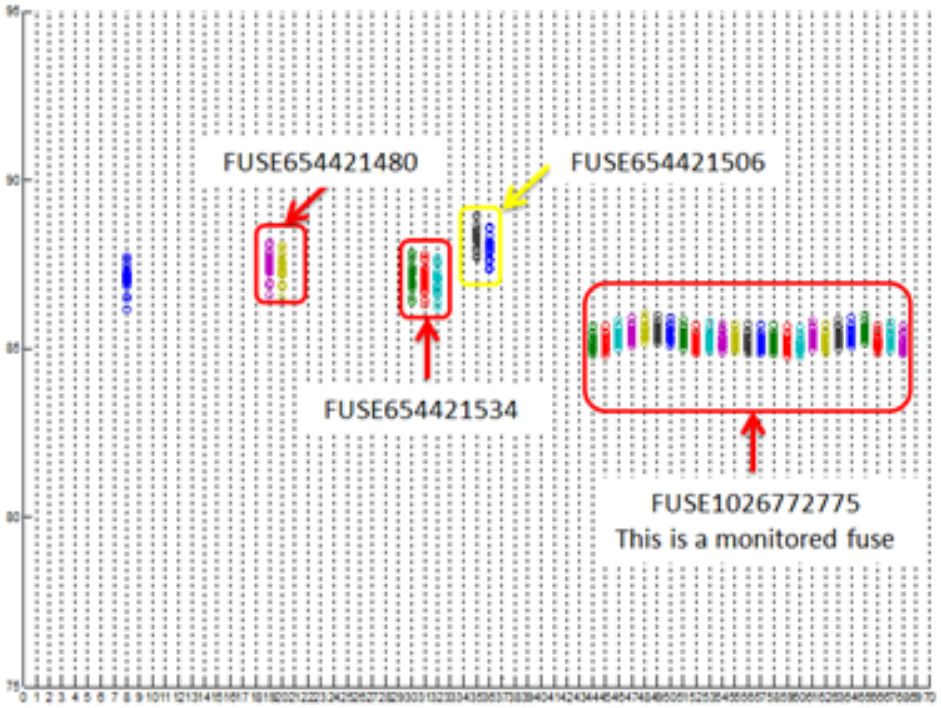

Figure C.9: P4597 - Results for 10% Load Variation (Showing Nodes with over a 75% Match)

9. '2A7744'
10. '2A7744'
11. '1T9382'
12. '1W0136'
13. 'P4592'
14. 'P4591'
15. 'P4585'
16. '2A7818'
17. '2A7818'
18. '2A7819'
19. '2A7820'
20. '1248612'
21. 'P4582'
22. 'P4582'
23. '2A4990'
24. '2A4990'
25. 'P4585'
26. 'P4580'
27. 'P4579'
28. 'P4579'
29. 'P4579'
30. 'P4594'
31. 'P4597'
32. 'P4597'
33. '1002869'
34. 'P4602'
35. '1C6533'
36. 'P4665'
37. '1254860'
38. '2050951'
39. '2050951'
40. '2050952'
41. '1130074'
42. '1254532'
43. '1254532'
44. '1254532'

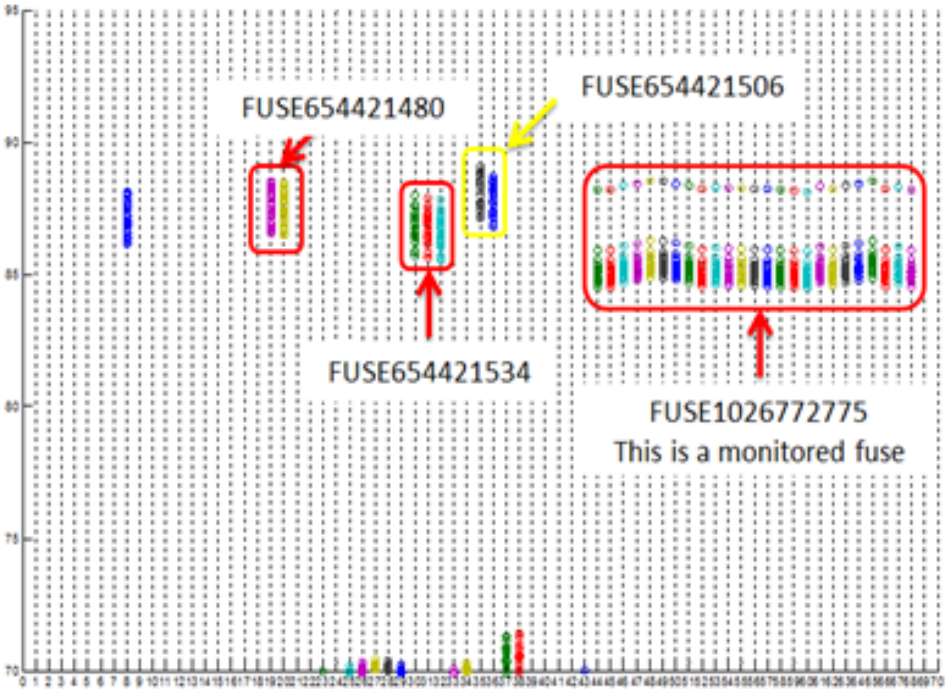

Figure C.10: P4597 - Results for 20% Load Variation (Showing Nodes with over a 75% Match)

45. '1254533'
46. '1254531'
47. '1254531'
48. '2051112'
49. '1254531'
50. '2050966'
51. '1254530'
52. '1254528'
53. '1254859'
54. '2050943'
55. '2050943'
56. '2050952'
57. '2050963'
58. '1254539'

C.7 Fault at 1002850 - Possibly Faulted Nodes

1. 'P4539'
2. 'P4464'
3. 'P4464'
4. 'P4464'
5. 'P4467'
6. '1002844'
7. 'P4476'
8. 'P4476'
9. 'P4477'
10. 'P4464'
11. 'P4489'
12. 'P4490'

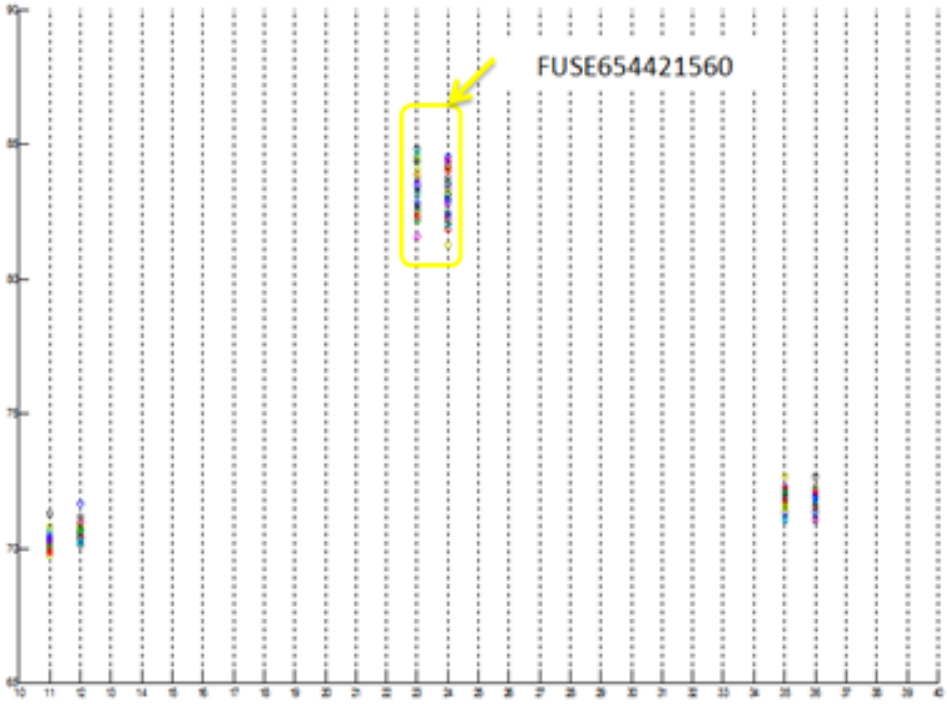

Figure C.11: 2A4990 - Results for 10% Load Variation (Showing Nodes with over a 65% Match)

13. 'P4490'
14. 'P4490'
15. '1Y9574'
16. '1Y9574'
17. 'P4489'
18. 'P4492'
19. 'P4492'
20. 'P4492'
21. 'P4412'
22. 'P4412'
23. 'P4416'
24. 'P4416'
25. 'P4417'
26. '1002850'
27. 'P4420'
28. 'P4110'
29. 'P4109'
30. 'P4401'
31. 'P4400'
32. 'P4398'
33. 'P4396'
34. 'P4393'
35. 'P4392'
36. 'P4392'
37. 'P4384'
38. 'P4385'
39. 'P4385'
40. 'P4387'
41. 'P4391'
42. 'P4384'
43. 'P4383'
44. 'P4381'
45. 'P4381'
46. '1248615'
47. '1N4654'
48. 'P4545'

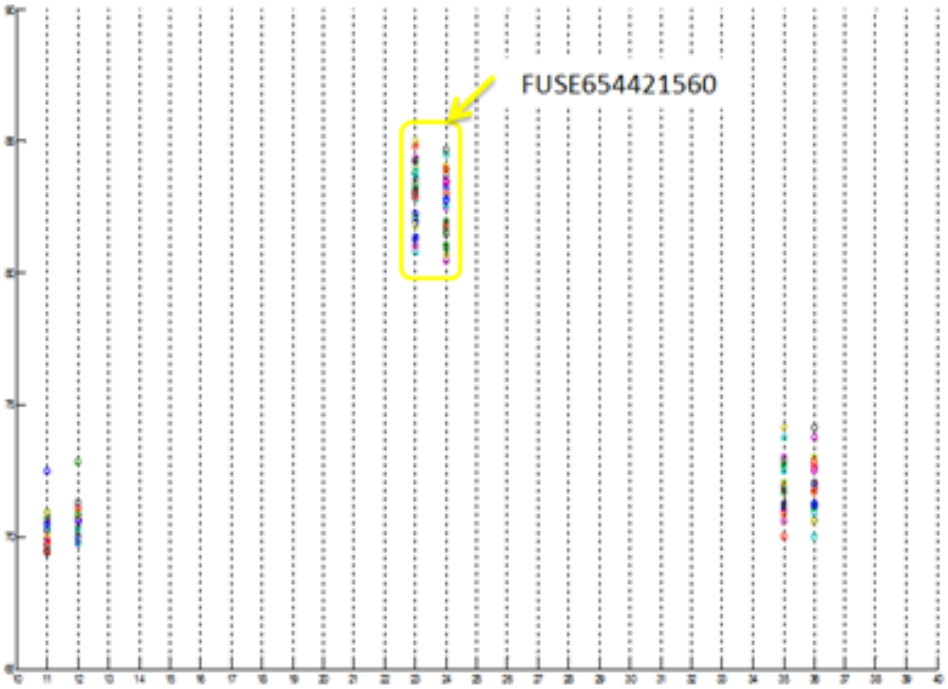

Figure C.12: 2A4990 - Results for 20% Load Variation (Showing Nodes with over a 65% Match)

49. 'P4550'
50. 'P4550'
51. 'P4566'
52. 'P4566'
53. 'P4550'
54. 'P4552'
55. 'P4554'
56. 'P4550'
57. 'P4556'
58. 'P4560'
59. 'P4560'
60. 'P4609'
61. 'P4609'
62. '1209489'
63. '1209489'
64. '1209489'
65. '1209490'
66. 'R0711'
67. 'R0712'
68. 'P4609'
69. 'P4609'
70. 'P4614'
71. 'P4614'

C.8 Fault at 1254532 - Possibly Faulted Nodes

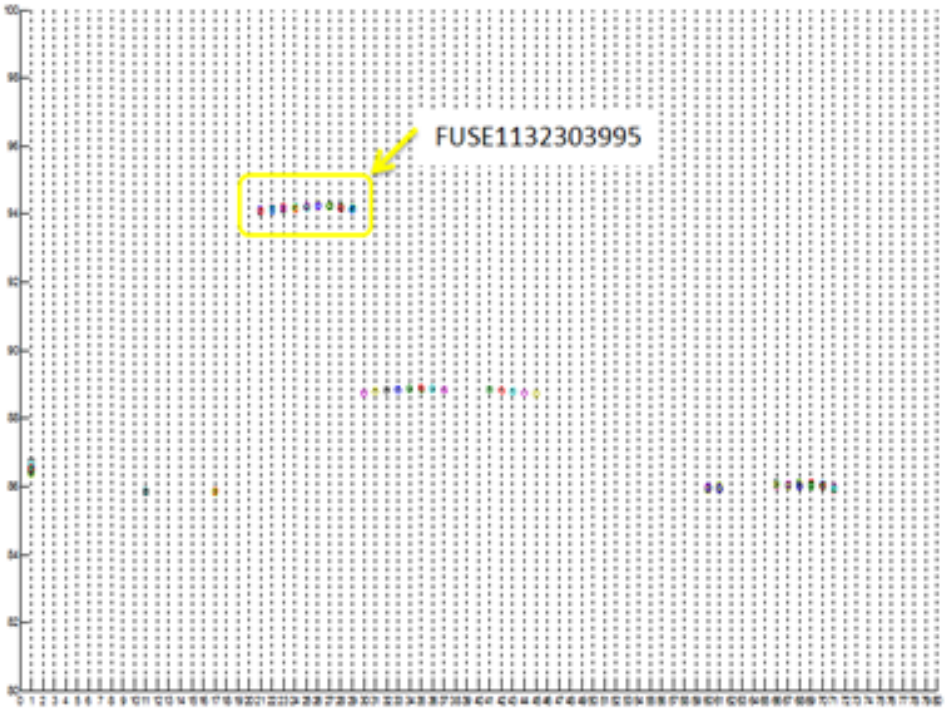

Figure C.13: 1002850 - Results for 10% Load Variation (Showing Nodes with over a 80% Match)

1. '1248681'
2. '1254468'
3. '1Y9416'
4. '1216626'
5. '1216626'
6. '1216626'
7. '1216628'
8. '1216629'
9. '1216630'
10. '1216630'
11. '2A7744'
12. '2A7744'
13. '1T9382'
14. '1W0136'
15. 'P4624'
16. 'P4592'
17. 'P4591'
18. 'P4585'
19. '2A7818'
20. '2A7818'
21. '2A7819'
22. '2A7820'
23. '1248612'
24. 'P4582'
25. 'P4582'
26. '2A4990'
27. 'P4585'
28. 'P4580'
29. 'P4579'
30. 'P4579'
31. 'P4594'
32. 'P4597'
33. 'P4597'
34. '1002869'
35. 'P4663'
36. '1C6533'

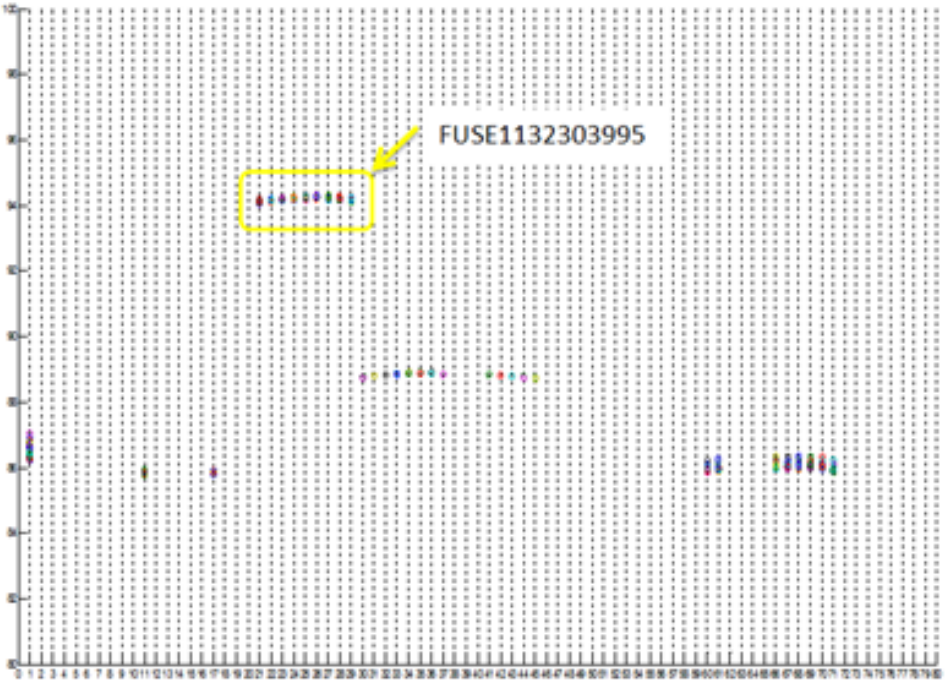

Figure C.14: 1002850 - Results for 20% Load Variation (Showing Nodes with over a 80% Match)

37. 'P4665'
38. '1248663'
39. '1248664'
40. '1254860'
41. '2050951'
42. '2050951'
43. '2050952'
44. '1130074'
45. '1254532'
46. '1254532'
47. '1254532'
48. '1254533'
49. '1254531'
50. '1254531'
51. '2051112'
52. '1254531'
53. '2050966'
54. '1254530'
55. '1254528'
56. '1254859'
57. '2050943'
58. '2050943'
59. '2050952'
60. '2050963'
61. '1254539'

C.9 Fault at 1254804 - Possibly Faulted Nodes

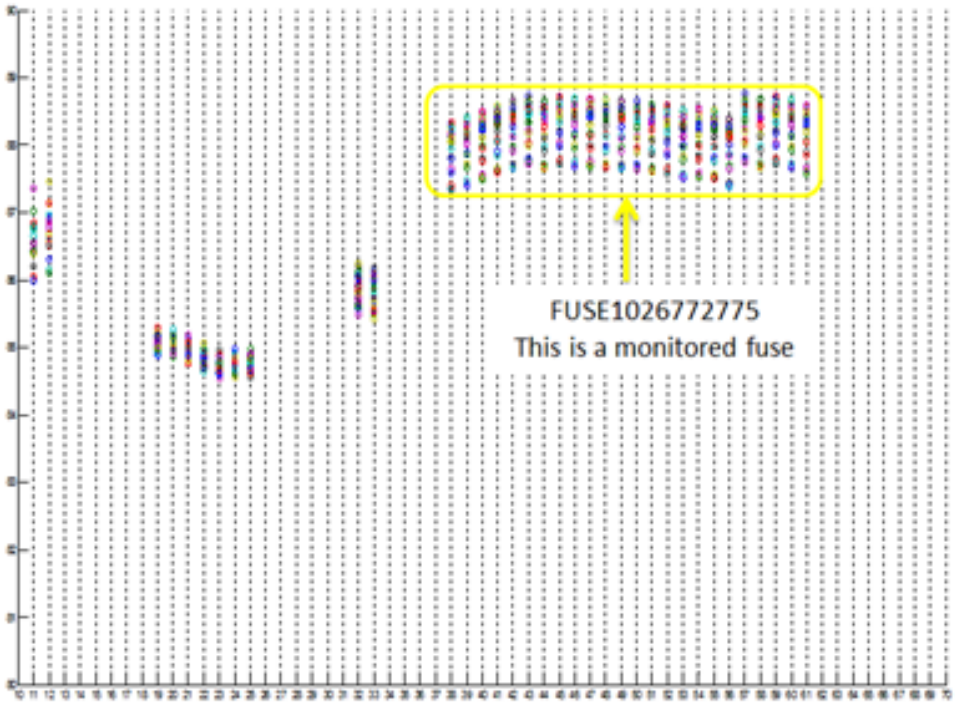

Figure C.15: 1254532 - Results for 10% Load Variation (Showing Nodes with over a 80% Match)

1. 'P4496'
2. 'P4496'
3. 'P4498'
4. 'P4498'
5. 'P4502'
6. 'P4508'
7. 'P4509'
8. 'P4509'
9. 'P4513'
10. 'P4513'
11. 'P4515'
12. 'P4375'
13. 'P4238'
14. 'P4236'
15. 'P4236'
16. 'P4235'
17. 'P4235'
18. '1279017'
19. '1279017'
20. '1279017'
21. '1279017'
22. 'N7970'
23. 'N7970'
24. 'N7955'
25. 'N7955'
26. 'N7955'
27. '1063586'
28. 'N7972'
29. 'N7972'
30. 'N7973'
31. 'N7974'
32. 'N7974'
33. '1L5936'
34. 'N7976'
35. 'N7976'
36. 'N7977'

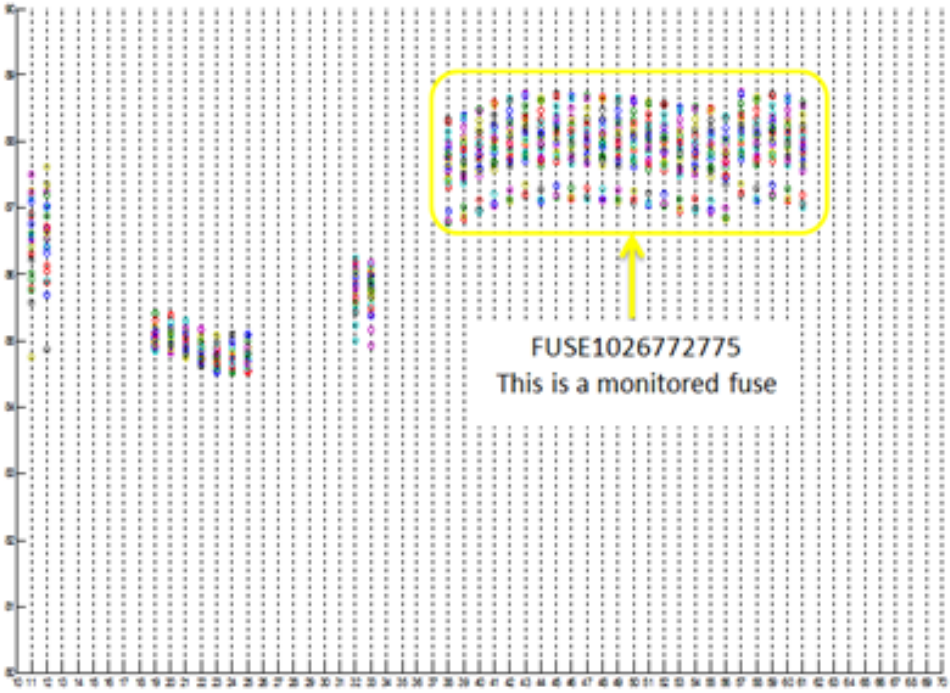

Figure C.16: 1254532 - Results for 20% Load Variation (Showing Nodes with over a 80% Match)

37. 'P4240'
38. 'P4241'
39. 'P4241'
40. 'P4247'
41. 'P4247'
42. '1254805'
43. '1254804'
44. '1254804'
45. 'P4266'
46. '1254806'
47. '1254806'
48. '1254807'
49. '1254808'
50. '1254809'
51. 'P4268'
52. '1267645'
53. '1254568'
54. 'P4616'
55. 'P4616'
56. 'P4618'

C.10 Fault at P4622 - Possibly Faulted Nodes

1. 'P4498'
2. 'P4513'
3. 'P4515'
4. 'P4515'
5. 'P4520'
6. 'P4522'
7. 'P4522'
8. '1L5936'

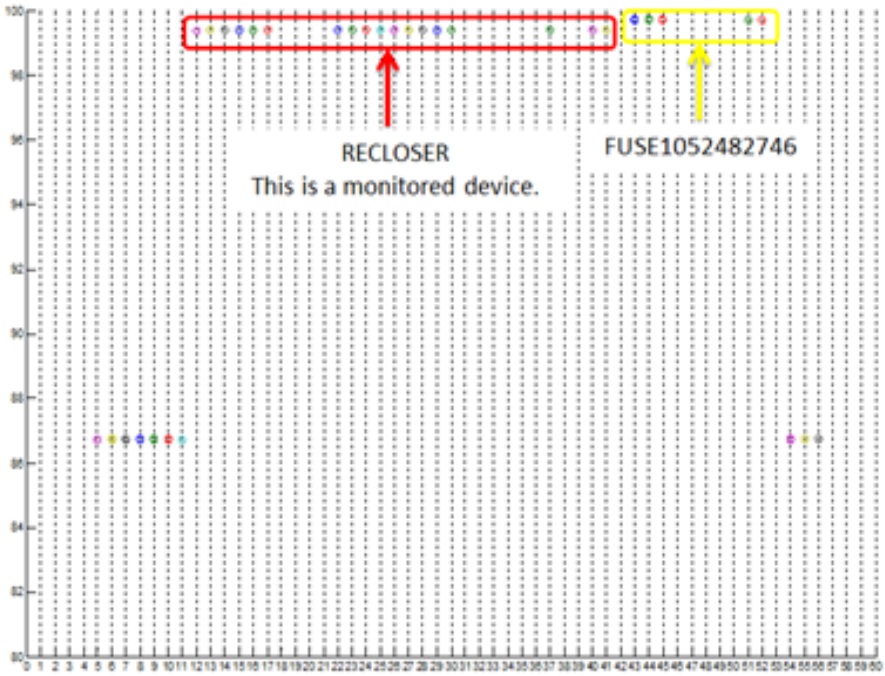

Figure C.17: 1254804 - Results for 10% Load Variation (Showing Nodes with over a 80% Match)

9. 'N7976'
10. 'N7976'
11. 'N7977'
12. 'N7977'
13. 'P4618'
14. 'P4619'
15. 'P4622'
16. 'P4622'

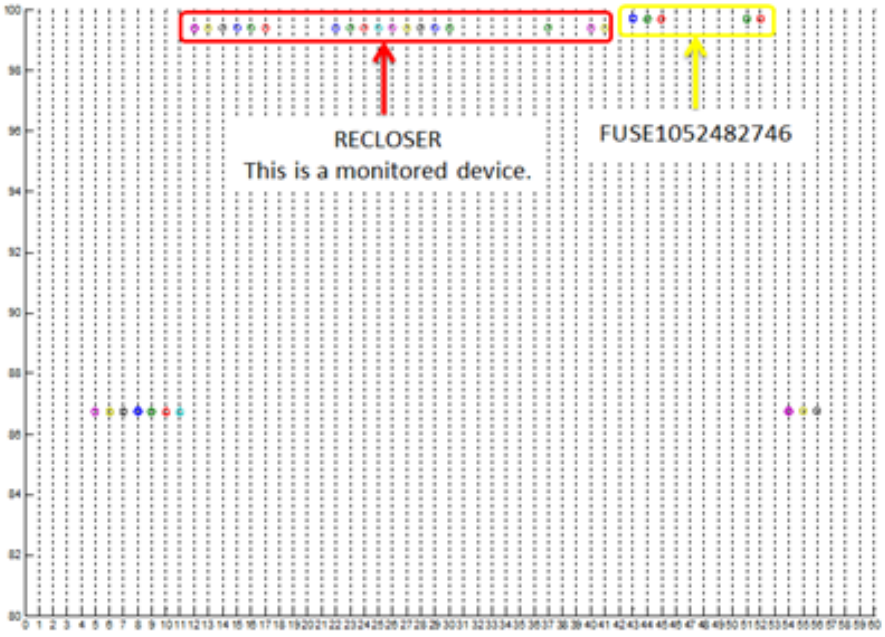

Figure C.18: 1254804 - Results for 20% Load Variation (Showing Nodes with over a 80% Match)

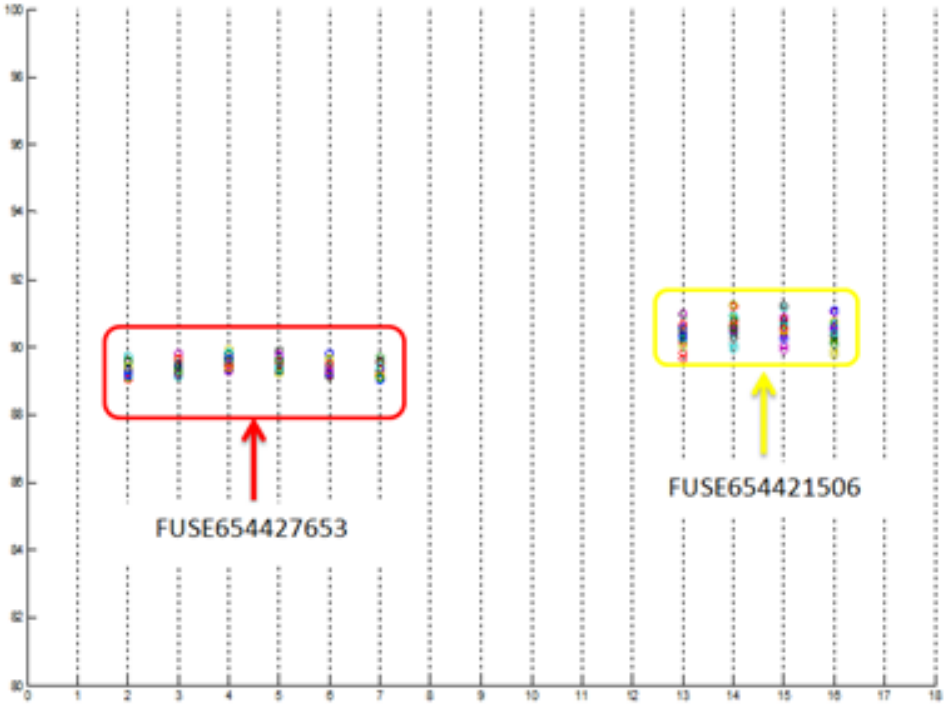

Figure C.19: P4622 - Results for 10% Load Variation (Showing Nodes with over a 80% Match)

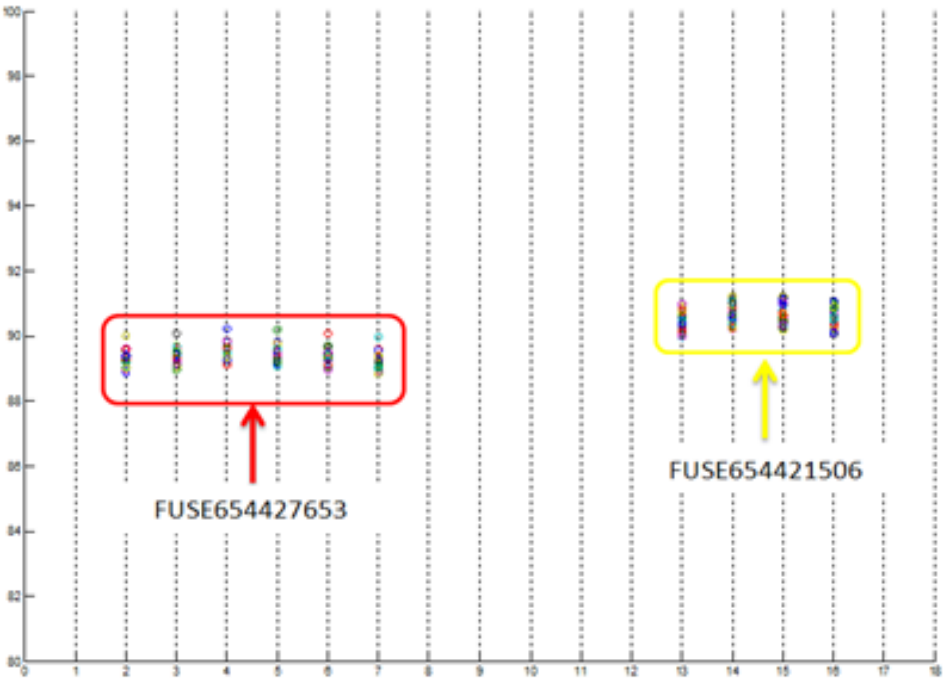

Figure C.20: P4622 - Results for 20% Load Variation (Showing Nodes with over a 80% Match)

Chapter D Data Requirements for FLA

In addition to the current waveforms, the program has certain data it needs so that it can work on the input to generate the expected output. Also, this data needs to be in a certain format so that the program may be able to access it. This section details the additional data that the program needs and the format that this data needs to be in.

D.1 Pre-requisite

A model of the system on which power flow studies and short circuit analysis can be performed. In this case DEW and CYME were used for the modelling and for the power flow and short circuit studies.

D.2 Data from Short Circuit Analysis

The first thing the program needs is the results from the short circuit analysis. These give the magnitudes of the currents observed by the measurement devices for a fault at every node in the system. In this case we create a table with the fault current values at the substation breaker and the two other locations where PQ monitors have been placed. This is stored in a Microsoft Excel file. The format of the table is shown in figure D.1.

As can be seen the table only shows the fault currents associated with a single type of fault. Additional tables are created that list the fault current magnitudes for the various types of faults on the various phases. The formats for the tables is as shown in figure D.2.

	A	B	C	D	E
1	4047	47	17	2C0234	
2	2940	2763	11	1254532	
3	2969	31	9	P4597	
4	2303	37	12	P4622	
5	2966	31	8	2A7818	
6	2859	37	11	2A4990	
7	2896	30	6	P4459	
8	2784	24	3	1002850	
9	2516	29	5	1254804	

Figure D.1: Fault Currents Table for Single Line to Ground Fault

Single Line to Ground Fault									
Current at Substation			Current at Measurement 1			Current at Measurement 2			Node
Line to Line Fault									
Current at Substation - Phase 1	Current at Substation - Phase 2		Current at Measurement 1 - Phase 1	Current at Measurement 1 - Phase 2		Current at Measurement 2 - Phase 1	Current at Measurement 2 - Phase 2		Node
Three Phase Fault									
Current at Substation - Phase 1	Current at Substation - Phase 2	Current at Substation - Phase 3	Current at Measurement 1 - Phase 1	Current at Measurement 1 - Phase 2	Current at Measurement 1 - Phase 3	Current at Measurement 2 - Phase 1	Current at Measurement 2 - Phase 2	Current at Measurement 2 - Phase 3	Node

Figure D.2: Format in which the Data is Stored in the Excel file

D.3 Data from load Flow Analysis

Based on the results of the power flow, an estimate can be obtained as to the amount of current that flows through each protective device under normal operating conditions. This information can be used to pinpoint protective devices that may have operated by measuring the drop in load. Therefore this data is stored in a file. Also, this data is updated based on the pre-fault conditions thereby giving the most accurate power flow results based on the pre-fault loading conditions. Refer figure D.3.

	A	B	C	D
1		A	B	C
2	FUSE654421375	2.43	0	21.51
3	FUSE1147838285	0	0	5.21
4	FUSE1156623368	0	0	0.02
5	FUSE654420956	0.68	0.68	0.68
6	FUSE654420971	0	3.47	0
7	FUSE1027155228	0	6.94	0
8	FUSE654421362	0	0	15.61
9	FUSE759763407	0	0	6.94
10	FUSE654421349	0	0	5.19
11	FUSE654421245	0	0	1.73
12	FUSE654421124	1.13	2.86	1.13
13	FUSE654421111	0	18.52	0
14	FUSE654421070	0	0	5.2
15	FUSE654421271	0	0	0

Figure D.3: Load Flow Current Data

D.4 Time Current Characteristics

From the algorithm, it is clear that the program attempts to identify the device that operated to isolate the fault. For this, the program needs to know the time-current characteristics for all the protective devices in the system. These are stored in a separate Microsoft Excel file. Refer

figure D.4.

	A	B	C	D	E	
1	Current		Fuse		Fuse	
2			FUSE654421375		FUSE1147838285	
3	1	10000	0.014667	10000	0.013512	1
4	2	9333.26	0.014948	6750.29	0.013553	9
5	3	8676.21	0.01522	6120.14	0.013675	8
6	4	7929.46	0.015574	5621.42	0.013785	7
7	5	7276.03	0.015952	5251.87	0.013896	7
8	6	6743.54	0.01634	4906.62	0.014021	6
9	7	6306.53	0.01677	4506.79	0.014205	5
10	8	5827.48	0.017315	4168.62	0.014391	5
11	9	5499.1	0.017771	3890.68	0.014608	5
12	10	5132.46	0.018368	3682.47	0.014785	4
13	15	4877.27	0.01887	3454.18	0.015008	4
14	20	4584.06	0.019699	3236.8	0.01525	4
15	25	4312.79	0.020524	3039.17	0.015481	3
16	30	4049.47	0.02149	2867.91	0.015699	3
17	35	3817.46	0.022547	2658.03	0.016016	3
18	40	3602.34	0.023703	2480.81	0.016389	3
19	45	3375.64	0.025168	2338.68	0.016753	3
20	50	3144.28	0.027101	2229.07	0.01704	2
21	55	2958.21	0.028835	2116.12	0.017437	2
22	60	2763.74	0.031174	2025.03	0.017771	2
23	65	2564.04	0.033838	1905.2	0.018313	2

Figure D.4: Data for the Fuse Curves

D.5 List of Protective Devices on the Feeder

This file lists the various protection devices present in the system. Refer figure D.5.

D.6 Zones of Protection for each Protective Device

As the program tries to organize the likely faulted nodes under their respective protective devices, it looks up this file to find which protective device's zone a particular node is in. This file lists the various protective devices with the corresponding nodes that it protects. From thus file a basic idea about the topology of the system can be obtained. Each protective device is said to protect only those nodes that are directly in its zone of protection. Refer figure D.6.

	A
1	FUSE654421375
2	FUSE1147838285
3	FUSE1156623368
4	FUSE654420956
5	FUSE654420971
6	FUSE1027155228
7	FUSE654421362
8	FUSE759763407
9	FUSE654421349
10	FUSE654421245
11	FUSE654421124
12	FUSE654421111
13	FUSE654421070
14	FUSE654421271
15	FUSE654421258
16	FUSE755195154

Figure D.5: List of Protective Devices

	A	B	C
1	FUSE654421375	FUSE1147838285	FUSE1156623368
2	P4653	P4641	1279022
3	P4654		
4	P4655		
5	P4660		
6	P4662		
7	P4663		

Figure D.6: Zones of Protection for the Devices

D.7 Additional Measurements

Once measurements from additional locations were included in the program, to aid in the elimination of unlikely nodes the program needs to know which protection devices are downstream of the point of measurement. This file lists the devices that are downstream of a particular point of measurement. The format for this data is given in figure D.7.

Measurement Point	Measurement Point
List of Downstream Protective Devices	List of Downstream Protective Devices

Figure D.7: Additional Measurements